RD6 (FLYSUB) Consortium

Project leaders

Brookhaven National Lab: Craig Woody

Florida Tech: Marcus Hohlmann

Lawrence Livermore National Lab: Mike Heffner, Ron Soltz

Stony Brook University: Klaus Dehmelt, Thomas Hemmick

University of Virginia: Nilanga Liyanage

Weizmann Institute of Science: Alexander Milov, Ilia Ravinovich

Yale University: Richard Majka

RD6 TRACKING/PID CONSORTIUM

PROGRESS REPORT & FUNDING REQUEST

FY 2014 AND 2015

We report on the progress of the RD6 consortium to date as the continuation in evaluating our highly successful sector test of forward arm tracking plus ring imaging Cherenkov detector and propose R&D work for a TPC capable to be performing as a central tracker and more in an EIC detector.

TABLE OF CONTENTS

Contents

TABLE OF CONTENTS

Overview and Collaboration Status

OVERVIEW

After a very successful sector test in October 2014 at Fermilab the groups of the RD6 consortium are continuing their effort to further develop and push forward detector technologies based on the experience gained from the test beam.

COLLABORATION STATUS

Recently, interest has peaked in the development of a fast TPC for the EIC. As a result new groups have already joined our consortium and others are discussing membership. Presently one group from Lawrence Livermore National Laboratory (headed by Ron Soltz and Mike Heffner) and one from the Weizmann Institute of Science (headed by Alexander Milov and Ilia Ravinovich) have joined the consortium with specific interests in the development of a large TPC. Two other groups are currently in negotiation to join, also with interests in the development of the TPC for central tracking at EIC.

As a new development, Florida Tech and U. Virginia plan to join forces with Bernd Surrow, et al., from the EIC RD2012-3 effort in designing and constructing the next detector prototype for the EIC forward tracker using entirely domestically sourced materials (see p.34 below for more details). For now, each of the three groups will formally continue within their own EIC RD project, but will collaborate with each other.

Progress Reports Past

WHAT WAS PLANNED FOR THIS REPORTING PERIOD?

Brookhaven National Lab group

There were two main efforts planned for the first half of 2014. The first was to finish the analysis of the test beam data taken with the minidrift GEM detector at Fermilab in October of 2013, and the second was to finalize the design and begin construction of the TPC/Cherenkov prototype detector. However, an opportunity occurred to obtain more test beam data with the minidrift detector due to the beam test of our EMCAL and HCAL prototype detectors at Fermilab in February of 2014. Since we did not complete all the measurements we wished to make with the minidrift detector in 2013, we took this opportunity to take more data and complete those measurements.

Our main plans for the TPC/Cherenkov prototype were to finish the mechanical design and the design of the field cage and readout board. We also need to identify, and eventually obtain, a system of readout electronics that could be used for full testing of the prototype.

Florida Tech group

The main task for this period was a detailed analysis of tracking data taken at the Fermilab beam test in Oct 2013 to study the performance of a large GEM prototype detector with zigzag strip readout – in particular to measure the angular resolution.

Stony Brook University group

The RICH prototype has been highly successfully tested in two test-beam campaigns (SLAC and Fermilab). It has been used with large pad readout which showed limited position resolution. For overcoming this limitation we were proposing to begin work on a resistive charge division scheme to allow high precision single photon position resolution measurements.

The results of the two test-beam campaigns are being prepared for publication in a peer-reviewed journal like NIM A.

University of Virginia group

The main goal was the analysis of the large amount of data taken during the test beam at Fermilab in October 2014 and to study the performance of the largest 2D triple GEM detector ever built.

Exploration of new ideas for the improvement of the performances and construction of the second generation EIC GEM prototype.

Yale University group

3 Coordinate GEM

The major activity during this period and the next period is the continuing analysis of the data from the Fermilab Test Beam with the 800 μm pitch 3 coordinate chambers and electrical tests on the 600 μm pitch boards.

Hybrid Gain Structures for TPC Readout

This effort was only recently funded but we planned to start initial measurements on the basic parameters of interest for a combined GEM + Micromegas (MMG) chamber. Of critical interest for use of the hybrid gain structure in a TPC are positive ion backflow (IBF), energy resolution and stability.

WHAT WAS ACHIEVED?

Brookhaven National Lab group

The minidrift GEM detector was taken back to Fermilab and set up along with the silicon telescope in the MT6.1 test beam area and tested for approximately one week in early February. The data taking run went very smoothly and we obtained more data with the detector at different angles and orientations.
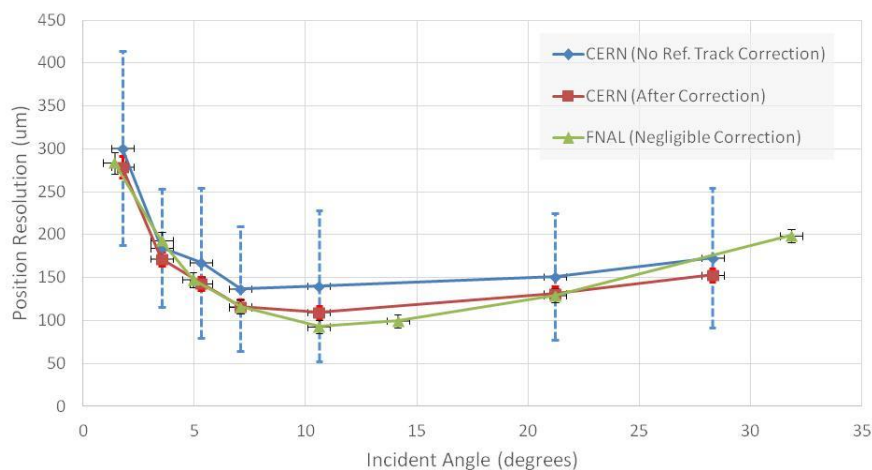

Figure 1 Position resolution of the minidrift detector using the track segment found in the detector as a function of angle for data taken at CERN and Fermilab. Resolutions are shown before and after unfolding the error on the extrapolated track from the two beam tracking systems.

The analysis of the new Fermilab data is nearly complete and it agrees well with the data taken at Fermilab in 2013 and at CERN in 2012. One major improvement in the Fermilab data was that the error on the extrapolated track from the beam tracking system was much smaller than in the CERN data. The CERN tracking system used a set of micromegas detectors that was located approximately 2 m away from the minidrift detector. This introduced a large error ($\sim$ 100 mm) due to the long extrapolation in determining the position of the track in our detector which had to be unfolded in order to determine its resolution. At Fermilab, the beam tracking system consisted of a high precision silicon telescope located only $\sim$30 cm from our detector, which made a negligible contribution to the position error. Figure 1 shows the position resolution of the minidrift detector before and after unfolding the error on the extrapolated track for the CERN and Fermilab data. The final position resolution agrees very well in the two cases, but the error from the unfolding is significantly reduced in the Fermilab data.

The position resolution shown in Figure 1 was computed using the vector track segment measured in the minidrift detector. It shows that at small angles (< 10°), the position resolution is very poor, which is due to the fact that there are not enough measurements along the track to determine the vector. For small angles, a simple charge weighted centroid gives much better position resolution. However, one can combine the two

methods and obtain good position resolution for all angles. Figure 2 shows a comparison of the position resolution for the charge weighted centroid method, the vector method, and using an algorithm that weights these two. Using the weighting algorithm, it is possible to obtain a position resolution ~ 100 μm for angles up to 20° and below 200 μm up to more than 30°. This constitutes an enormous improvement over the position resolution one would obtain with a conventional GEM tracking detector at larger angles (which would use only the centroid method), and makes this type of detector very attractive for tracking applications at EIC, particularly at forward and intermediate rapidities.
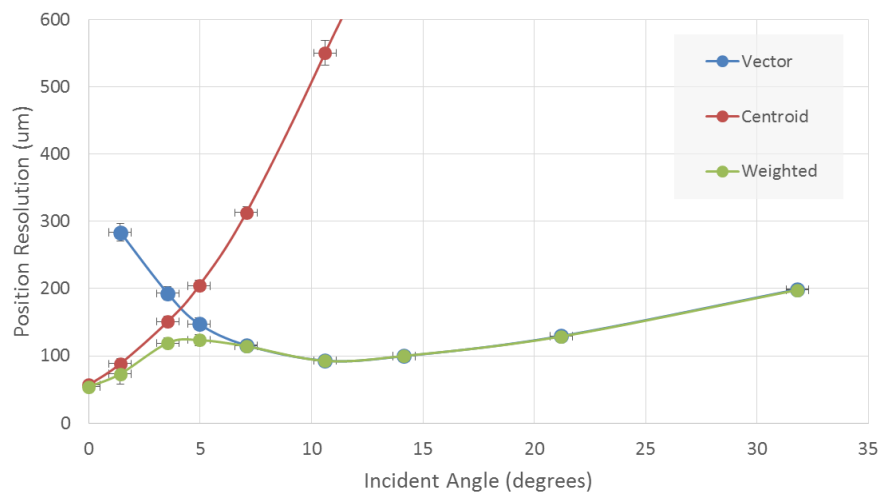

Figure 2 Position resolution for three different methods of coordinate determination: Simple charge weighted centroid method; Vector method using vector track segment measured in the minidrift detector; Position determined with a weighting algorithm using both the centroid and vector measurements.

The data shown in the plots above were taken with a Compass style readout plane with a XY strip readout. The detector was oriented at 45° in phi relative to the beam axis, such that neither the X nor the Y strips were aligned along the axis of rotation for measuring the angular dependence. We also took data with the detector oriented with the X and Y strips aligned along the axis of rotation. In this case, only one coordinate at a time is used to compute the vector. This allows us to study the intrinsic position resolution of each readout plane separately. Figure 3 shows a comparison of the resolution obtained with each individual readout plane compared to the resolution for each plane in the 45° orientation, obtained by projecting out the separate resolutions for each view. The agreement is quite good and gives a measure of the intrinsic resolution of the vector method using the strips of the Compass style readout plane.
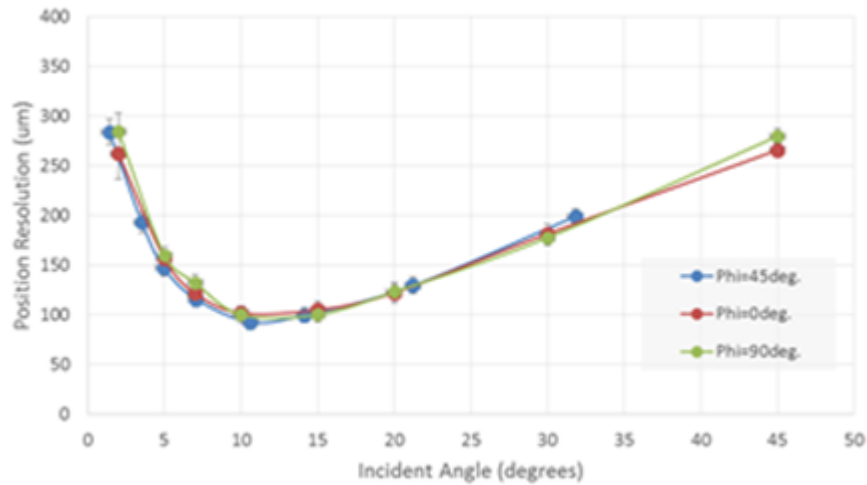
Figure 3 Position resolution of the individual X and Y readout planes of the Compass style readout plane measured in three different phi orientations: phi=0 deg. (Y-strips measured alone), phi=45 deg. (X and Y strips measured simultaneously), and phi=90 deg. (X-strips measured alone).

With the vector reconstruction method it is also possible to measure the angular resolution that can be achieved with the minidrift detector. Figure 4 shows the angular resolution as a function of angle, and shows that a resolution of ~ 12 mrad can be achieved for angles greater than ~ 15°. This can also provide valuable information for track finding in various EIC detectors.

Figure 4 Angular resolution measured with the minidrift detector using the vector reconstruction method.

We also took data with a readout plane consisting of 2x10 mm chevron pads in order to study the resolution of the readout plane we plan to use for our TPC prototype detector, and the analysis of these data is currently under way.

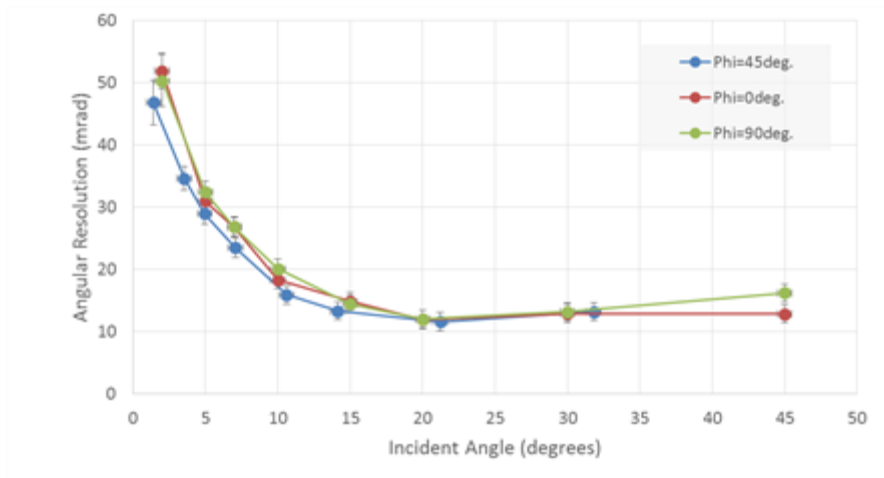Progress was also made on the design of the prototype TPC/Cherenkov detector, although this was somewhat limited due to the fact that we focused of our attention on the completion of the studies of the minidrift detector during this period. The mechanical design of the various components of the prototype detector is shown in Figure 5. A number of refinements were made to the design and many of the components are now ready for fabrication. Figure 6 shows the final design of the field cage which is ready to be produced. We further developed the design of the readout plane, which would use the same type of chevron pads as we tested with our minidrift detector, and this is now ready for a detailed layout of the PC board. Most of the mechanical components of the support stand and gas enclosure are also ready for fabrication.
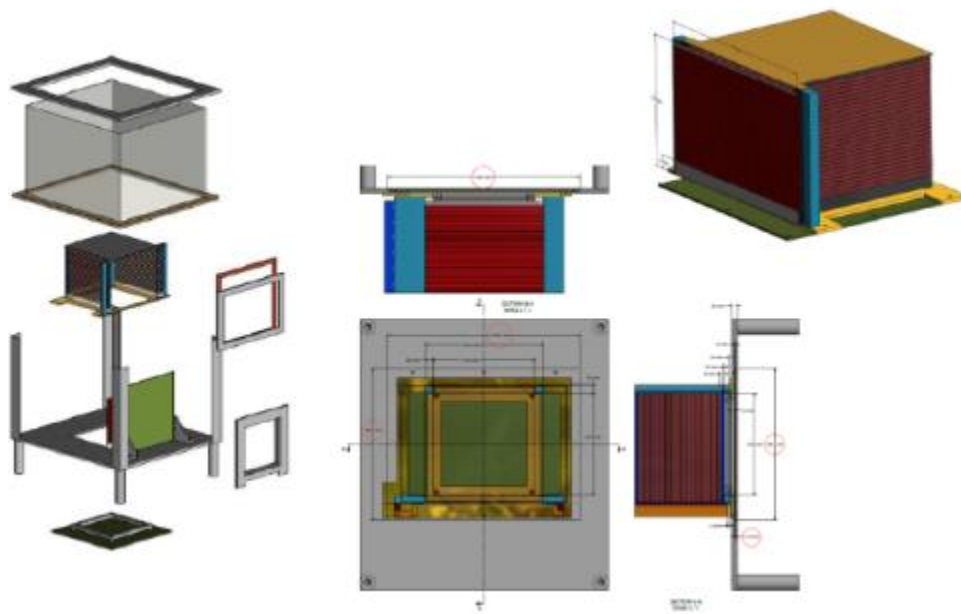

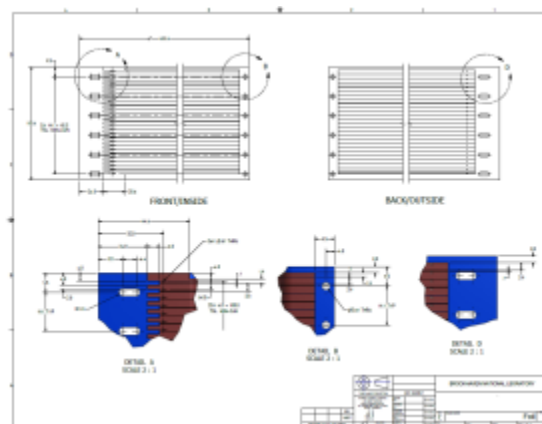**Figure 5 3D model of the prototype TPC/ Cherenkov detector.**

Figure 6 Final design of field cage kapton foil ready for fabrication.
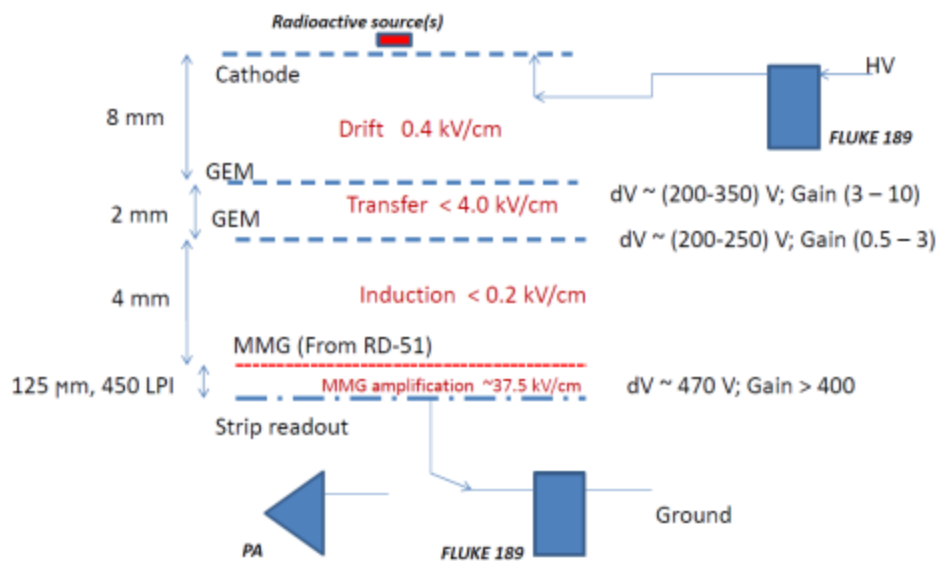

Figure 7 Setup with double GEM plus micromegas detector for measuring ion back flow.
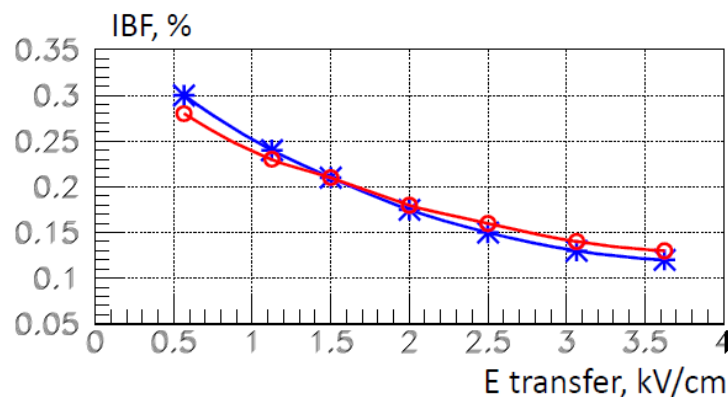
Figure 8 Ion back flow measured with double GEM plus micromegas readout. Gas was Ne/CO$_2$ (90/10). Red points were taken with an ^{55}Fe source and blue points were taken with a ^{90}Sr source.

We also continued our studies of reducing ion back flow in the TPC. One attractive approach for this is to use a combination of GEM detectors to provide gain and a micromegas detector as the last stage to reduce the ion feedback. This takes advantage of the inherently low ion back flow provided by the micromegas combined with the stable operation of the GEM detectors. Figure 7 shows the setup that was used to test this combination. Figure 8 show the percentage of ion back flow as a function of the transfer field between the two GEMs. The ion back flow can be reduced to a level of almost 0.1% using this combination, which would greatly reduce space charge build up in the TPC and allow it to be used in a high rate environment such as EIC.

Florida Tech group

EIC post-doc Aiwu Zhang has been leading the data analysis effort focused on a one-meter trapezoidal GEM detector with a cost-conscious radial zigzag strip readout built at Florida Tech. A detection efficiency above 98% for charged particles is measured on the plateau. The cross-talk between zigzag strips is measured to be 5.5%. After aligning the GEM tracker internally and then aligning the trapezoidal 1-m GEM detector to the tracker using tracks, we measure the spatial resolutions of all GEM detectors. We study the non-linear response of the zigzag strips and develop corresponding correction functions. Applying those corrections substantially improves the angular resolution of the zigzag detector when operated on the efficiency plateau. After this correction, the detector achieves an angular resolution of ~170μrad, which corresponds to just 12% of the angular pitch of the zigzag strips.

Geometry: We briefly recall the readout geometry of the zigzag GEM detector. It is segmented into 8 η-sectors with 128 radial zigzag readout strips per sector. The pitch between two tips in the same strip is 0.5mm and the closest distance between tips in neighboring strips is ~0.1mm (Figure 9). The opening angle of the trapezoid is 10° and the angular strip pitch is 1.37mrad. This zigzag GEM detector can be fully read out with

only 8 APV hybrid chips; the zigzag design saves 2/3 of electronic channels and corresponding electronics cost compared to a standard straight-strip readout as used, e.g. in the CMS muon upgrade GEM detector, that this zigzag GEM detector is based on.
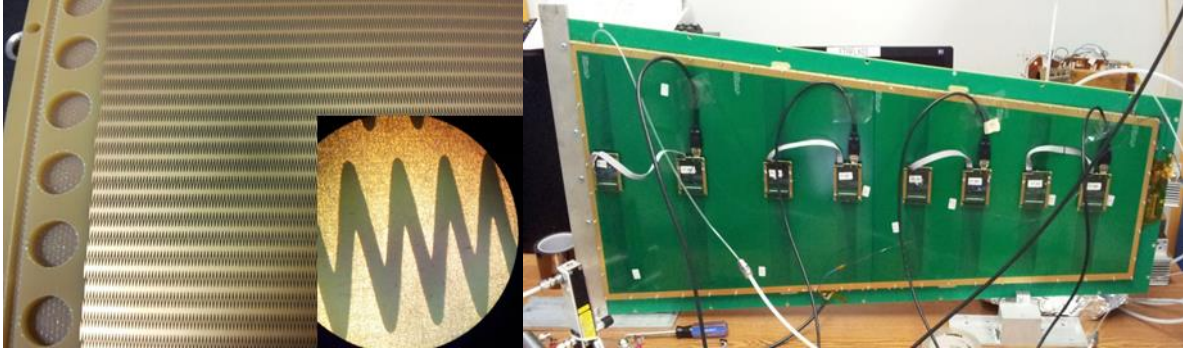
Figure 9 Left: A photo of the zigzag printed circuit readout board and a microscopic picture of the zigzag structure in the inset. Right: Trapezoidal GEM chamber with 3/1/2/1mm foil gaps and zigzag pcb fully instrumented with only 8 APV hybrids. Four HDMI cables (black) linked to an RD51 SRS DAQ read out the entire chamber.
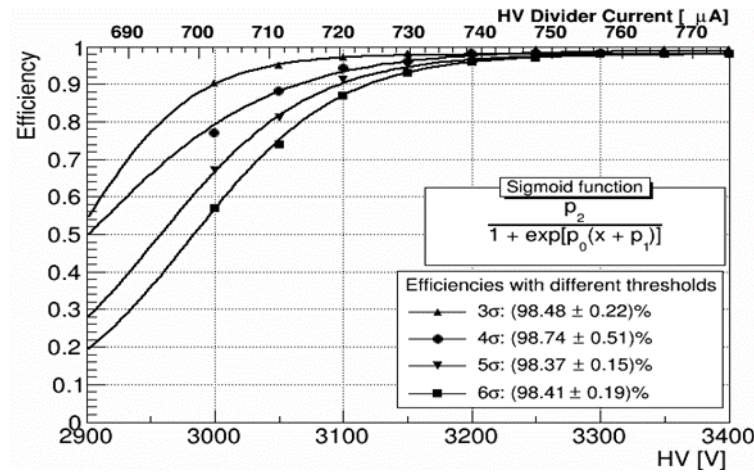
Figure 10 Detection efficiency vs. HV_{drift} in central sector 5 for different threshold cuts on the width of the pedestal distribution. Statistical errors are smaller than the marker sizes.

Efficiency Measurement: The detection efficiency of the zigzag GEM detector in mixed hadron beams was measured to be $(98.4 \pm 0.2)\%$ on the plateau when a 5σ threshold cut is applied to the measured strip charge to define a hit on a strip; here σ is the strip-by-strip width of the pedestal distributions. The efficiency as a function of HV is fitted with a sigmoid function. Figure 10 shows efficiencies for different threshold cuts; it demonstrates that the plateau efficiency is not affected significantly by the threshold.

Angular Resolution Measurement: Since the zigzag strips run in radial direction and measure the φ-coordinate, we need to perform the resolution study in polar coordinates. The first step in this measurement is an alignment of the standard 10cm × 10cm GEM trackers that have a Cartesian x-y strip readout. The trackers are first aligned to each other in Cartesian coordinates. Events with a single cluster observed in each tracker are used for the alignment. Any strip multiplicity is allowed in the strip clusters including single-strip clusters. We iterate through a succession of relative offsets and rotations around the beam axis until the residual means from track fits are very close to zero and the χ² of the track fits are minimized. The resolution is then calculated as the geometric mean of the widths of exclusive (σ_{ex}) and inclusive (σ_{in}) residuals: $\sigma = \sqrt{\sigma_{ex} \times \sigma_{in}}$, where exclusive (inclusive) means that the probed detector is excluded (included) when fitting the tracks. Figure 11shows that tracker resolutions in X and Y directions are 50-70µm in the 120GeV proton data; they are found to be 70-80µm in the wider mixed-hadron beam.
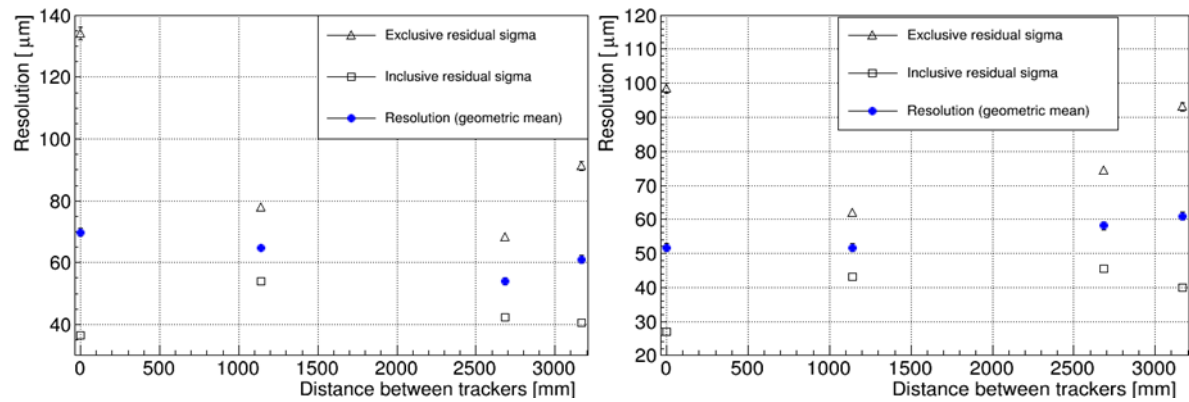
Figure 11 Exclusive and inclusive residual widths and spatial resolutions (blue) for the four reference GEM trackers in X (left) and Y (right) directions obtained with 120GeV proton data. The resolution is calculated from the geometric mean of the residuals.

Figure 12 (Left) Schematic diagram for transformation of the Cartesian tracker coordinates into the natural polar coordinate system of the zigzag GEM detector, which has the vertex of the trapezoid in its origin. (Right) Example of inclusive residual in the φ coordinate fitted to a double Gaussian for the first tracker with X_offset = 2m and Y_offset = 0m using 120 GeV proton beam data. The residual core width is 14 µrad.

Figure 13 Spatial resolutions (blue) of the four trackers in r (left) and φ (right) coordinates for X$_{offset}$ = 2m and for Y$_{offset}$ = 0m (examples) with 120GeV proton data.

The tracker hit positions must next be transferred to the polar coordinate system that is naturally given by the geometry of the large zigzag detector with the vertex of the trapezoid used as the origin of the polar system (Figure 12 left). The tracker tracks are then refit in those coordinates. As an example, if the offsets are taken as X$_{offset}$ = 2000mm and Y$_{offset}$ = 0mm, Figure 12 (right) shows the resulting inclusive track-hit residual distribution of the first tracker in the φ coordinate with proton data; for this particular detector the residual width is observed to be 14μrad. Overall, in this example the tracker resolutions are found to be ~70μm in the r coordinate and 25-30μrad in the φ coordinate (Figure 13), which is consistent with the residuals obtained in Cartesian coordinates since, e.g. 30μrad × 2m = 60um.

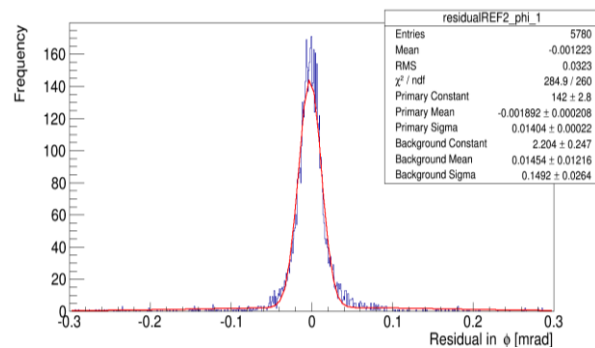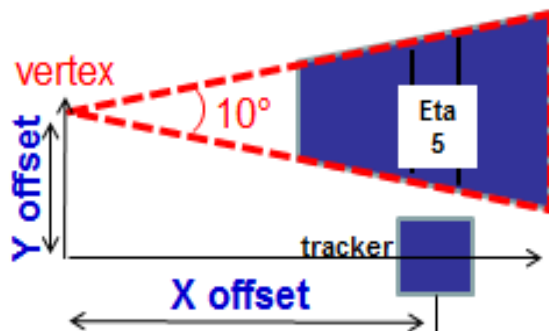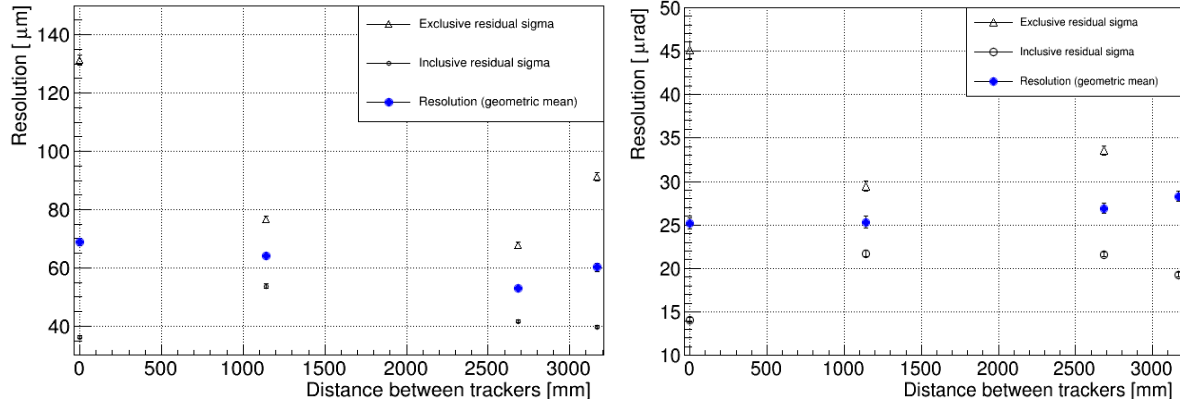In the polar coordinate system, the φ-coordinate of the center of each zigzag strip in the large trapezoidal detector is simply given by $\varphi_{zigzag} = -0.5 * \alpha + n * \alpha/(128 - 1)$, where $\alpha = 10°$ is the opening angle of the trapezoidal shape and n $= 0, 1, \cdots, 127$ is the strip number. The φ-position of a zigzag-strip cluster is initially determined from the barycenter, or centroid, of the strip cluster using the strip charges as weights.

For transforming the Cartesian tracker coordinates into the polar coordinate system, we need to find the correct X-offset and Y-offset from the new origin to the center of the tracker (Figure 12left) using the tracks in the φ coordinate. This has to be done for each test configuration. Note that since the trackers are already internally aligned, the centers of the individual trackers already match, so there is only a single pair (X$_{offset}$, Y$_{offset}$) of offsets to be found for each configuration. The idea behind our alignment procedure is that any misalignment will shift the residual means away from zero and will increase the residual widths when fitting tracks in the φ-coordinate with hits in the trapezoidal GEM.

We use a two-fold iteration loop to find the X and Y offsets for each data taking configuration. First, we keep a fixed X$_{offset}$ value and step through Y$_{offset}$ values with a fixed step of 0.2mm within a reasonable physical range, then change to another X$_{offset}$ value with a step of 1mm and vary the Y$_{offset}$ again until all X$_{offset}$ values have been covered. For each (X$_{offset}$, Y$_{offset}$) pair, all tracks are fitted in the φ-coordinate including and excluding the φ-hit in the zigzag detector and the inclusive and exclusive residuals for the zigzag GEM

detector are histogrammed. We record residual means and widths, as well as the mean χ^2 of the tracks in the φ coordinate.

We use a three-step procedure to find the best estimate of the offsets. Figure 14shows an example of this procedure for the data recorded in the central η-sector 5 of the zigzag GEM at 3300V. For a given X_{offset} value we record that Y_{offset} which produces a well-centered φ-residual for the zigzag detector with a mean of zero (Figure 14left). Then, for a given Y_{offset}, we plot the residual widths as function of X_{offset} and find the X_{offset} value that minimizes the residual width using a parabolic fit (Figure 14center). This yields two sets of (X_{offset}, Y_{offset}) pairs that are plotted as two curves. The (X_{offset}, Y_{offset}) values for which those two curves intersect is taken as the best estimate of the alignment offsets (Figure 14 right). Best (X_{offset}, Y_{offset}) pairs based on track-χ^2 are also plotted and confirm the results.

Finally, it is not guaranteed that tracker and zigzag detector are installed without a relative rotation in the X-Y plane (Figure 15left). Since aligning the zigzag GEM detector also requires matching the X direction to the trackers so that all calculations of φ are correct, the rotation angle of the zigzag GEM detector needs to be checked. The mean χ^2 of tracks in φ vs. rotation angles is a parabola and the angle can be calculated from the minimum; it is very close to zero (Figure 15 right).
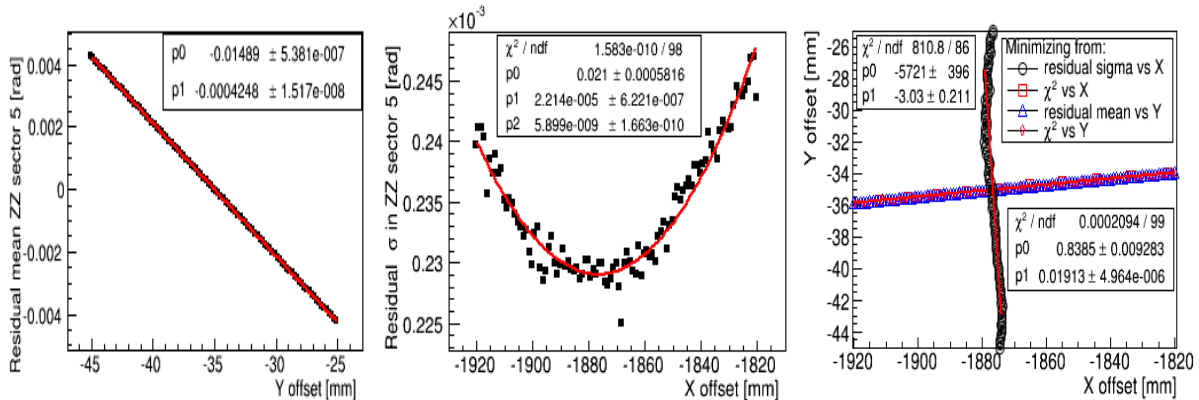
Figure 14 Optimization of X and Y offsets for trackers with beam impacting on zigzag GEM in central ⬜-sector 5. (Left) At fixed X_{offset}=-1876mm, the residual mean vs. Y_{offset} curve is a line, the best Y_{offset} offset at this X_{offset} point is calculated from requiring that the residual mean be equal to zero: Y_{offset}=-35.05mm. (_Center_) At fixed Y_{offset}=-35mm, the residual width vs. X_{offset} is a parabola, the best X_{offset} is calculated from the minimal point of this parabola: X_{offset}=-1876.6mm. (_Right_) Scatter plots of best (X_{offset}, Y_{offset}) points from residual mean vs. Y_{offset} and residual sigma vs. X_{offset}, as well as plots of χ^2 vs. X_{offset} and χ^2 vs. Y_{offset}, which strongly overlap with the former.
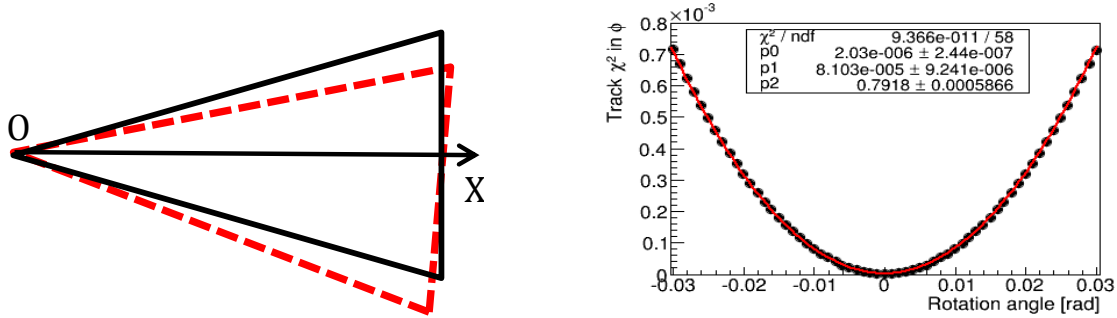
Figure 15 (Left) Schematic diagram for slight relative rotation of the zigzag detector. (Right) Mean χ^2 of tracks in φ direction vs. rotation angles for the same data as in Figure 14.

Once the X and Y offsets and the rotation angle are determined and fixed, exclusive and inclusive φ-residuals of the zigzag GEM detector are calculated. The angular resolution is then again determined from the geometric mean of the two residual widths. Figure 16 shows exclusive and inclusive residuals for the central η-sector 5 of the zigzag GEM detector operated at 3300V. The resulting measured resolution is 256μrad.

Figure 17 (left) shows the resolution in φ measured in central η-sector 5 of the zigzag GEM detector when operated at different high voltages. When all strip multiplicities including single-strip clusters are allowed ("Not cut" points in Figure 17), the angular resolution decreases as HV increases with the best resolution found to be ~240μrad. This figure also shows angular resolutions vs. HV for specific strip multiplicities. The resolution is found to be significantly better for clusters with exactly two strips hit (~210μrad at higher HVs) than for clusters with other strip multiplicities. The measured relative fraction of strip multiplicities as a function of HV is shown in Figure 17 (right). Figure 18 shows resolutions in different sectors of the detector. The resolutions show variations that reflect the known response non-uniformity of the chamber due to slight bending.
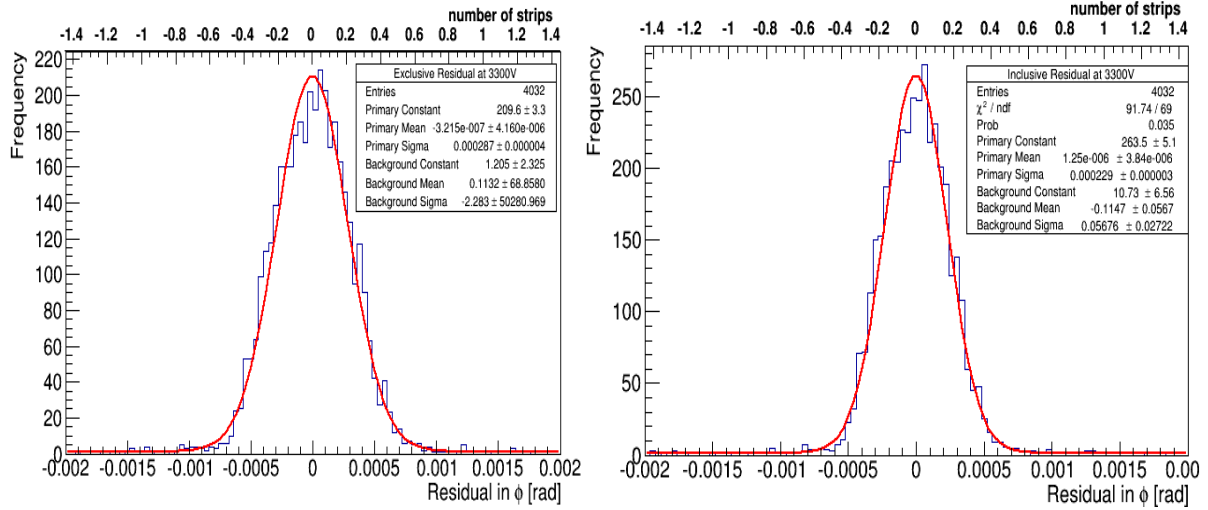
Figure 16 Exclusive (left) and inclusive (right) φ-residual distributions fitted with double Gaussians for central η-sector 5 of the zigzag GEM detector at 3300V after alignment but before corrections for strip response. The resulting measured φ-resolution is 256 μrad.

Figure 17 (Left) Angular resolutions measured in central ⏧-sector 5 of the zigzag GEM detector vs. HV_drift for different strip multiplicities of clusters after alignment but before corrections for strip response. (Right) Relative fraction of strip multiplicities vs. HV_drift.
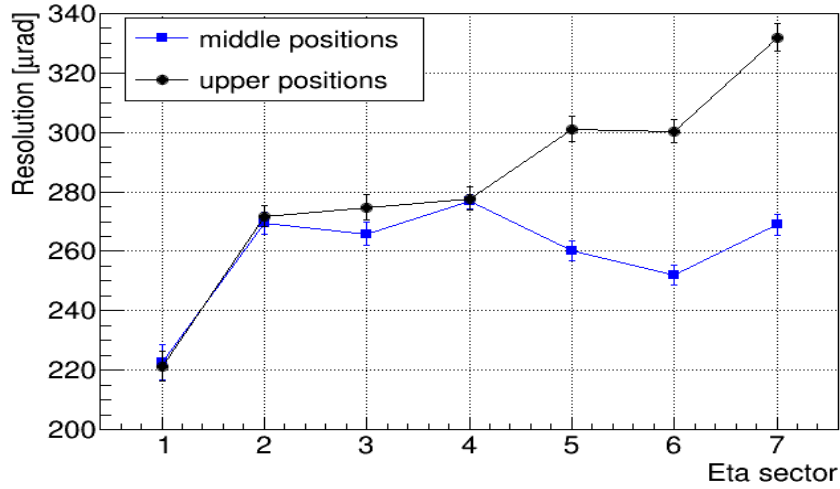
Figure 18 Measured angular resolutions in different sectors of the zigzag GEM at 3200V for two points in each sector with "middle positions" located along the center axis of the detector and "upper positions" near one edge. All strip multiplicities are used here.

In the above resolution studies, the basic barycentric method that gives the centroid of the strip clusters is used to reconstruct the positions of hits on the detector. When looking at the resulting strip positions for different cluster sizes in detail, we find that the measured centroid position distributions in the zigzag detector have a comb-like structure with peaks and gaps. In addition, the structures are different for different strip multiplicities, e.g. for N=2 and N=3 events (Figure 19). For N=2, the centroid tends to be in the center between the strips; for N=3 it tends to be near the center of the strip with the highest charge. This deviation from a uniform distribution reflects a non-linear strip response that typically exists in detectors with discrete readout strips. There are discussions of various methods of correcting this non-linear behavior of cluster positions based on centroids in the literature. Here, we implement a straightforward η-algorithm [1] to correct the centroid positions for clusters with strip multiplicities N=2, 3 and 4.
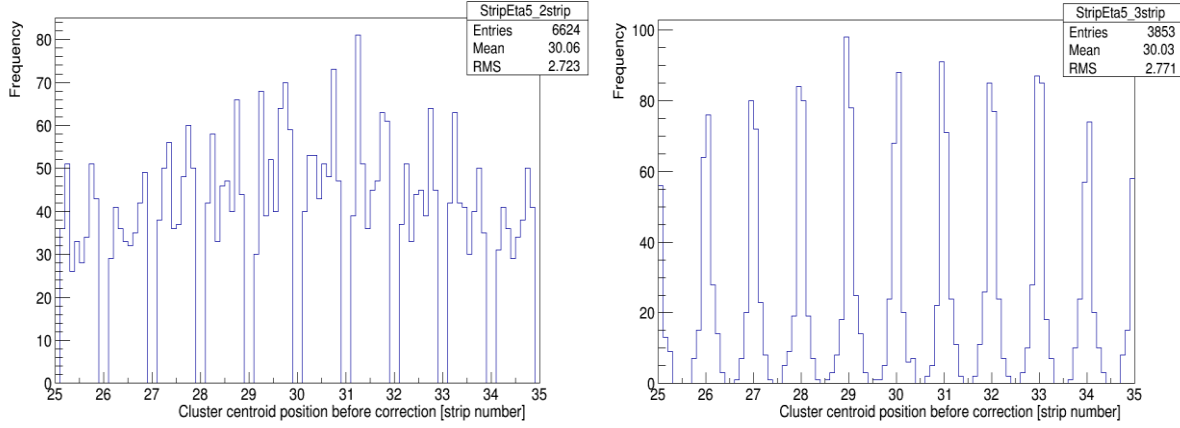
Figure 19 Cluster centroid position distributions for clusters with strip multiplicities N=2 (left) and N=3 (right) for the central η-sector 5 of the zigzag GEM.

The η-algorithm first defines a parameter η_N for each strip multiplicity (N=2, 3 and 4):

$$\boldsymbol{\eta_N = s_{centroid} - s_{maxQ}} \qquad \text{(Eq. 1)},$$

where $s_{centroid} = \sum \frac{q_i s_i}{q_{tot}}$ is the centroid position in terms of strip number from the barycentric method. Here q_i is the charge collected by the ith strip in the cluster, s_i is the corresponding strip number, $q_{tot} = \sum q_i$ is the total charge in the cluster, and s_{maxQ} is the number of the strip with the maximum charge in the cluster. For each selected strip multiplicity N, an η_N distribution is produced, which is taken as the strip response function $h(\eta_N)$ for that strip multiplicity. The centroid position for each cluster is then corrected according to Eq.2 [1]:

$$\boldsymbol{s'_{centorid} = s_{maxQ} - 0.5 + \frac{\int_{-0.5}^{\eta'} h(\eta)d\eta}{\int_{-0.5}^{0.5} h(\eta)d\eta}} \qquad \text{(Eq. 2)}.$$
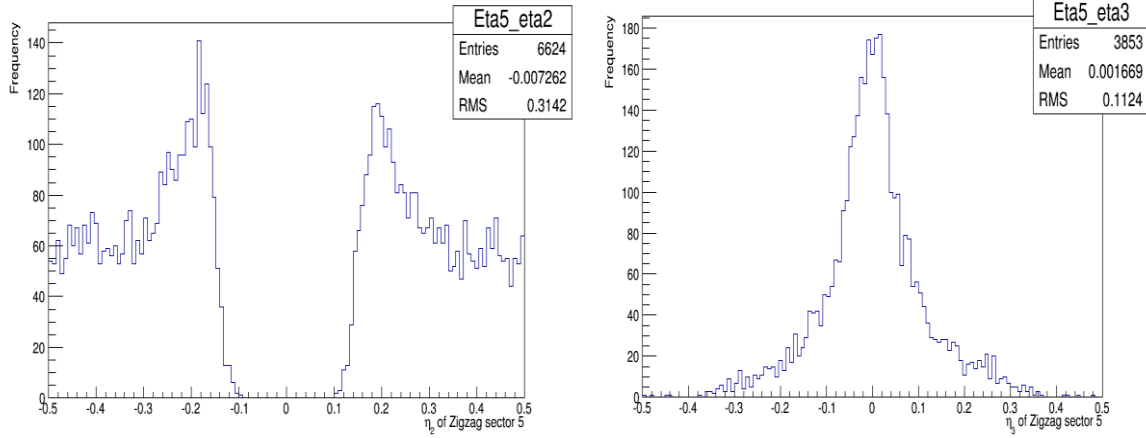
Figure 20 Measured strip response functions h(η₂) (left) and h(η₃) (right) for the zigzag GEM detector from HV scan data taken in central η-sector 5. In both cases, the central value zero is the center of the zigzag strip with maximum charge in the cluster.
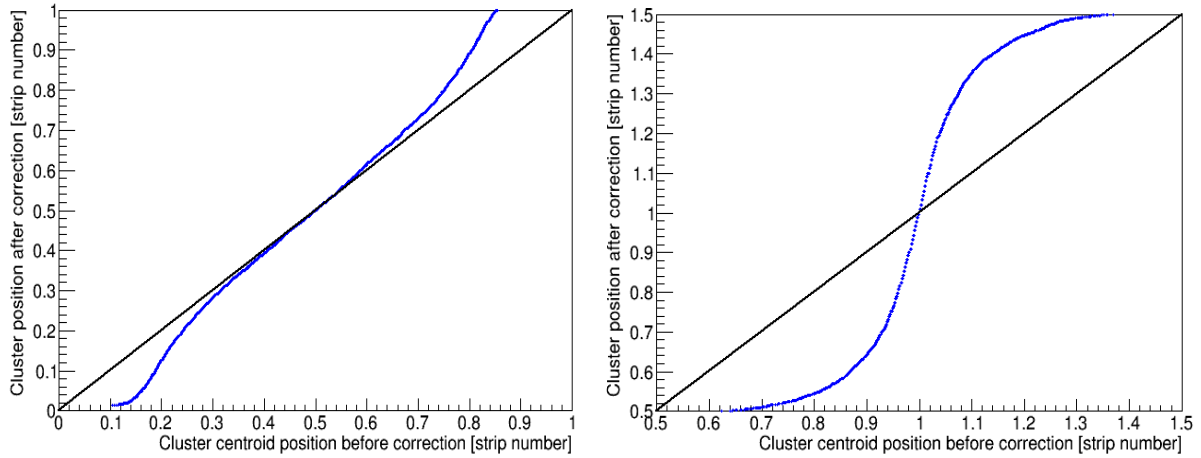
Figure 21 Position correction functions s'_centroid vs. s_centroid for clusters with strip multiplicities N=2 (left) and N=3 (right). For N=2 the strips are located at 0 and 1, while for N=3 the central strip with maximum charge is located at 1.

Figure 20 shows the $h(\eta_N)$ strip response distributions for strip multiplicities N=2 and N=3; the resulting position correction functions obtained by integration are shown in Figure 21. The $h(\eta_2)$ distribution has a gap in the middle while $h(\eta_3)$ peaks in the middle. This difference reflects the different centroid position distributions for N=2 and N=3 clusters shown in Figure 19. The position correction functions are similar to

sigmoid functions. It is obvious from the graphs that the non-linearity is larger for N=3 clusters than for N=2 clusters. This is consistent with the observation that the uncorrected resolution for N=2 cluster is better than for N=3 cluster. This implies also that larger corrections are needed for N=3 clusters than for N=2 clusters. Figure 22 shows the cluster position distributions after the corrections are applied for N=2 and N=3 clusters. Compared with Figure 20, the corrected distributions are less jagged, which means that the non-linear strip response has been reduced as expected.

Similar corrections are also applied to N=4 clusters; they yield results similar to the N=2 case. We then use all N=2, 3, and 4 clusters, which comprise more than 90% of all events on the efficiency plateau above 3250V (Figure 17 right), to recalculate the resolution for the HV scan data of the central η-sector 5 (Figure 23). For each HV point, the strip response histograms and response correction functions are calculated separately.

We find that at higher high voltage, i.e. on the efficiency plateau, the resolution improves significantly after correction, e.g. at 3400V drift voltage it goes from 235μrad to 170μrad after correction, i.e. it improves by 28%. At lower HV below the efficiency plateau, the resolutions deteriorate. A resolution of 170μrad corresponds to only 12% of the angular zigzag strip pitch of 1.37mrad. For comparison, for straight strips with binary readout the resolution is typically given by $1/\sqrt{12}$ = 29% of the strip pitch.
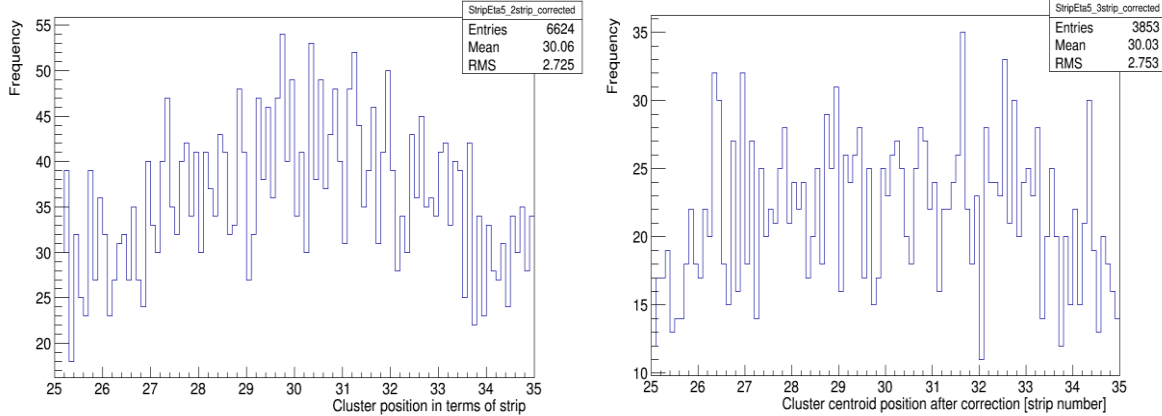
Figure 22 Position distributions for N=2 clusters (left) and N=3 clusters (right) after strip response correction for the central η-sector 5 of the zigzag GEM.
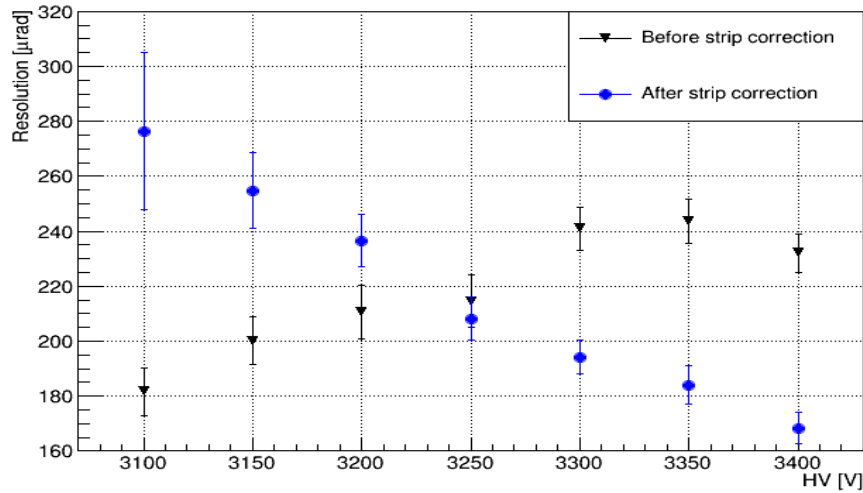
Figure 23 Angular resolutions vs. HV$_{drift}$ for the central η-sector 5 of the zigzag GEM after cluster positions are corrected (blue) for clusters with strip multiplicities N=2, 3, and 4 compared to the resolutions before cluster position corrections (black).

Cross-talk Measurement: We are also able to measure the cross talk between zigzag strips using the beam-test data. Due to a minor mistake that occurred during production of the zigzag readout board at the pcb company, two pins in each of the eight 128-channel Panasonic connectors, which are attached to the readout board and connect the zigzag strips to the APV hybrids, were accidentally connected to a large ground plane in the readout board instead of to zigzag strips. These pins correspond to strips 63 and 127. The large input capacitance presented by the plane to those two channels causes large noise as can be seen, for example, in the distribution of the pedestal widths for one of the sectors (Figure 24, left & center). These plots also show that channels 62, 64, and 126, which are adjacent to the two noisy channels, are victims of crosstalk as their pedestal widths are also slightly higher than the average pedestal width across all other strips.

We subtract the average pedestal width observed for strips not affected by crosstalk in quadrature from the pedestal width observed for the crosstalk victims and divide by the pedestal width of the corresponding crosstalk aggressor to estimate the relative crosstalk that exists among zigzag strips. The resulting distribution using several APVs and five different pedestal runs is shown in Figure 24 (right). We find that the mean crosstalk among the zigzag strips is (5.5 ± 0.2) % with an rms width of 1.3%. This analysis was performed by a Florida Tech undergraduate.
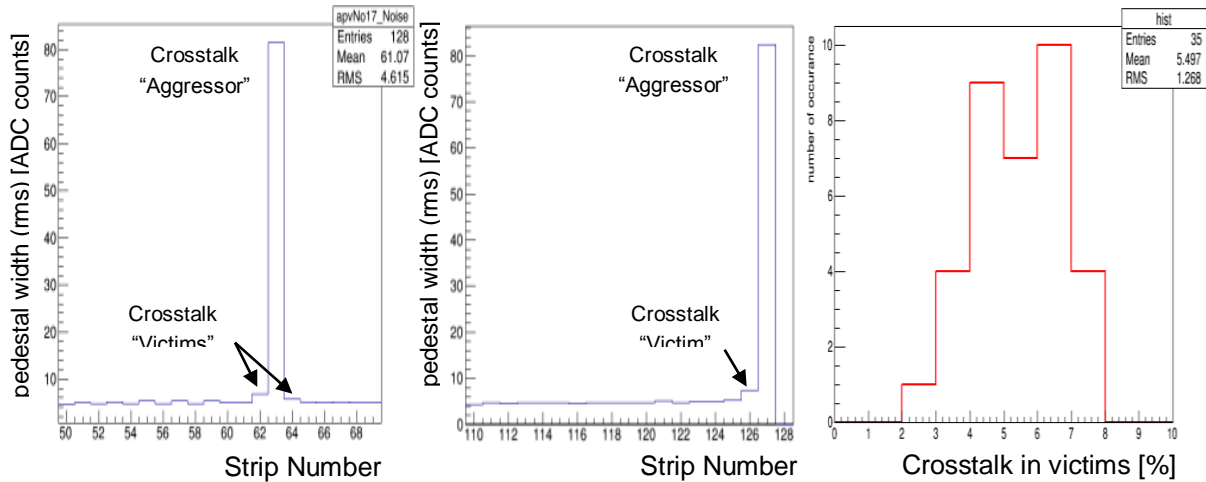
Figure 24 (Left and center) Pedestal widths (rms) observed for zigzag strips in the vicinity of two crosstalk aggressors. The adjacent strips are victims of crosstalk and show slightly higher pedestal widths. (Right) Crosstalk between zigzag strips measured with several APV hybrids and in a few pedestal runs.

Summary and Conclusion: The large GEM detector with radial zigzag strips achieves the high efficiency (>98%) for charged particles that is expected from a gaseous detector. Crosstalk among the zigzag strips is tolerable at an average level of 5.5%. The zigzag readout achieves an angular resolution of 170 µrad, i.e. 12% of angular strip pitch, with a small number of channels. This makes this readout considerably more cost-effective for large GEMs than conventional readout structures with straight strips.

We remind the reader that the geometry of an EIC forward tracker will presumably cover a radial range of ~0.1m < r < ~1m, which is different from the prototype radial range of 1.5m < r < 2.5m. If one uses the angular resolution measured with the current prototype to extrapolate the resolution in azimuthal φ-direction to the actual range of 0.1m < r < 1m, the resulting resolution is 170 µrad × (0.1m – 1m) = 17 µm – 170 µm. While this is a naïve calculation, and certainly a severe underestimate for the smaller radii, we can nevertheless conclude that the beam test results demonstrate that the measured performance of the zigzag readout is within a resolution of around 100 µm that is required in the azimuthal direction for a forward tracker of an EIC detector.

Related Activities: Aiwu Zhang presented the beam test results shown here in a contributed talk at the 2014 April meeting of the APS in Savannah, GA, and at the EIC users meeting at Stony Brook U. in June. An abstract featuring the results presented here was submitted to the 2014 IEEE NSS conference in Seattle.

Marcus Hohlmann has been participating in weekly meetings of a small task force that is working on developing a commercial domestic source for large GEM foils. The other members of this task force are Richard Majka (Yale) from this consortium, Bernd Surrow (Temple U., EIC RD2012-3 group), Matt Posik (Temple post-doc with B. Surrow), several representatives from TechEtch Corp., and Rui De Oliveira (CERN

workshops). So far, this effort has succeeded in enabling TechEtch to produce high-quality 10cm x 10cm and 30cm x 30cm GEM foils using CERN's single-mask etching technique. While all the technical work has been done at Temple (see EIC RD2012-3 report) and at Yale (see report from the Yale group in this document), Hohlmann has helped with guiding this effort and communicating with Rui De Oliveira at CERN.

Stony Brook University group

We have started developing software code that simulates and estimates the effect of pads based on resistive charge division regarding position resolution. The problem is based on electromagnetic first principles and has been identified and described by computer study work of an undergraduate student. The code has been started to be debugged and to be applied.

University of Virginia group

During the period of December 2013 to June 2014, the first EIC-GEM prototype built at UVa was tested with cosmic as well as in high energy hadron beam at the Fermilab Test Beam Facility (FTBF) in October 2013. The performance parameters of the detectors such as the gain uniformity, efficiency, charge sharing of the readout board have been studied. The chamber operates typically with Ar/CO_2 (70/30) gas mixture for the tests with a voltage applied to between 4kV and 4.2 kV on the HV divider. APV25 based Scalable Readout System (SRS) [2] by the RD51 collaboration [3] at CERN was used to readout the GEM chambers and ALICE DAQ and analysis software [4] used for the data acquisition.

Performances with the EIC-GEM prototype with cosmic data

Cosmic data was used to study the gain uniformity over the entire area of the chamber. The plot in Figure 25 2D cluster position reconstruction from cosmic data (left) and correlation plot (right) for ADC charge sharing between top layer strips vs. bottom layer strips of the readout. On the left shows the 2D cluster position distribution from cosmic data run; the lack of events at almost half of the chamber and the edge of the inner radius side of the chamber is due to the size limitations of the scintillator used to trigger the data acquisition. The narrow correlation plot with a slope equal 1 on the right indicates an equal sharing of the ADC between to top and bottom strips of the u/v readout board. The effect of the 300 μm wide spacers of the GEM frames support is clearly shown here on the two plots and represents a dead area with an approximate width of 2 mm.
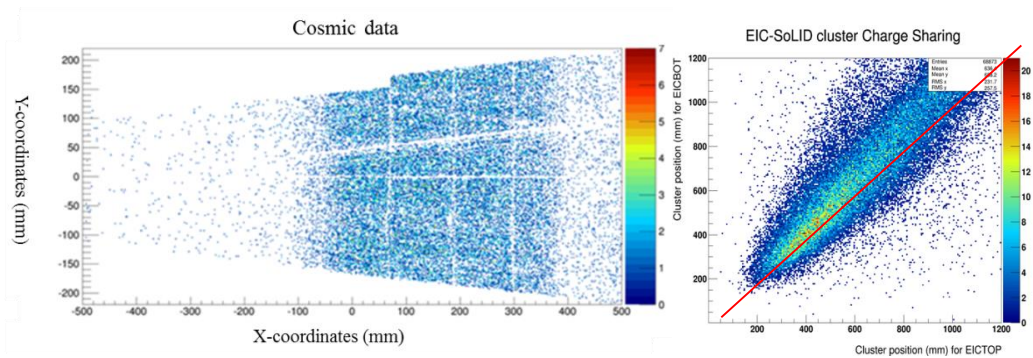
Figure 25 2D cluster position reconstruction from cosmic data (left) and correlation plot (right) for ADC charge sharing between top layer strips vs. bottom layer strips of the readout.

Performances with the EIC-GEM prototype at the FTBF test beam
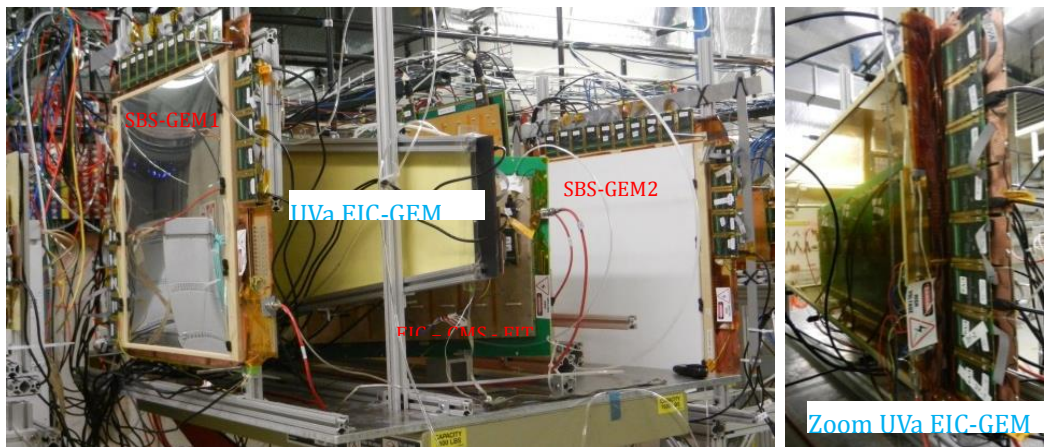
Figure 26 Large area EIC GEM on FTBF test beam setup (Oct. 2013)

Figure 26 shows UVa EIC-GEM prototype on the common MT6 setup between Florida Tech and UVa at the Fermilab Test Beam Facility (FTBF) in October 2013 as part of the large area GEMs for EIC Tracking and PID T-1037 beam test effort.
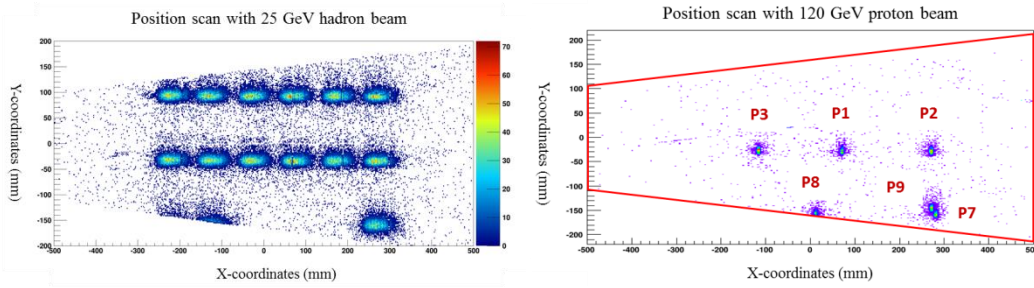
Figure 27 2D cluster position reconstruction from position scan with 25 GeV hadron beam (left) and 120 GeV proton beam (right).

Large amount of data was taken with the EIC GEM prototype with 120 GeV primary proton beam as well as lower energy (32 GeV, 25 and 20 GeV) secondary hadron beam composed mainly of kaons, pions and protons during the FTBF test beam. Figure 27 shows the beam profile reconstructed from cluster position from a position scan run with 25 GeV hadron beam (left) and with 120 GeV proton beam (right). We observed a very good uniformity of response over all the probe area of the chamber. Performances such as gain efficiency curves, cluster size distribution the position resolution and uniformity across the active area was also studied.

Efficiency

The left plot of Figure 28 shows efficiency curves against the voltage applied to the divider which correlation with the gain in the chamber is known and well calibrated. The efficiency is evaluated by the ratio between the number of good events in the chamber against the number triggered events recorded simultaneously in 3 trackers two upstream and one downstream the EIC chamber. The god and triggered events are defined by at least one cluster in each of both readout layers (top and bottom) of a given detector. Efficiency plateau above 97% is reached at 4100 V for cluster hit threshold equal to $3 \times \sigma$ cut with σ representing the width of the pedestal noise for each individual strip. A very good efficiency is still above 95% is observed for $5 \times \sigma$ cut.
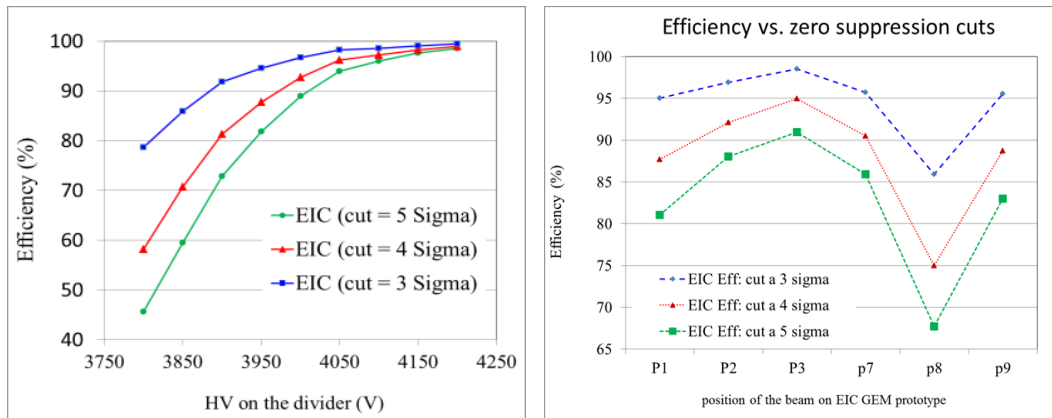
Figure 28 : Efficiency curves vs. HV applied on divider at different pedestal cuts (left); Efficiency vs. beam position on the prototype at different pedestal cuts (right).

On the right of Figure 28, one can see the efficiency at different locations on the chamber shown on the bottom plot of Figure 27. We observe no more than 3% variation of the efficiency at the probed location for $3 \times \sigma$ threshold, except for location P8 caused by the beam hitting the edge of the chamber with a large portion of the particle outside the active area of the chamber. At for $5 \times \sigma$ cut the variation of the efficiency reaches up to 10%.

Cluster size

The cluster size distribution defining average number of strips in the cluster event after pedestal cut is shown for both the top and bottom strips of the EIC-GEM prototype for a 3950 V with an average cluster size equal 2 for the top strips and 1.45 for bottom strips.
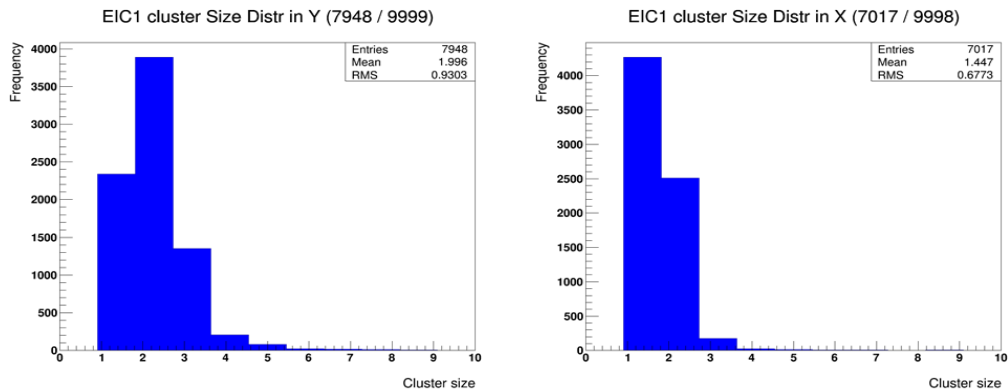
Figure 29 Cluster size distribution for top strips (left) and bottom strips (right).

The difference is explained by the higher capacitance noise of the bottom strips which led to smaller number of strips after the $5 \times \sigma$ cut. The plot on left of Figure 30 shows the cluster size against the voltage on the divider (chamber gain). At the operating voltages for the chamber between 4kV and 4.1 kV, the cluster size on the bottom electrode remained is smaller than 2 which affect limit the performance in term of the spatial resolution when the coordinate is calculated using the center of gravity of the cluster. A solution to this problem is narrower pitch and strips width in the next prototype. The cluster size at different location on the chamber is shown on the right with an overall good uniformity for the top strips and some important variation for bottom strips caused by the big variation of the strip length at different area in the chamber.
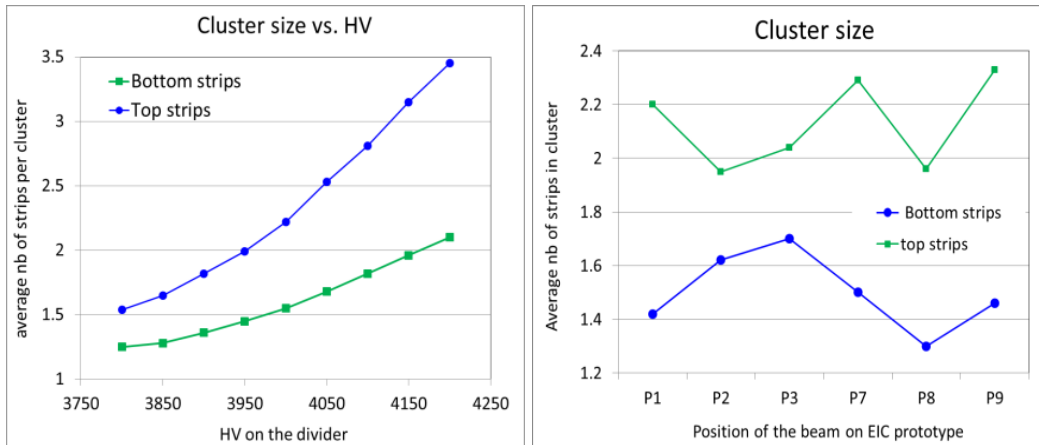
Figure 30 Cluster size vs. HV applied on divider for both top and bottom strips (left); cluster size vs. beam position on the prototype.

Charge sharing ratio

The charge sharing ratio between top and bottom strips is shown on Figure 31. The left plot shows an almost equal sharing with a ratio around 1.15 at different voltages (detector gain). We observed a small drop for high value of the voltage which is an indication of the saturation at high gain of the apv25 signal.
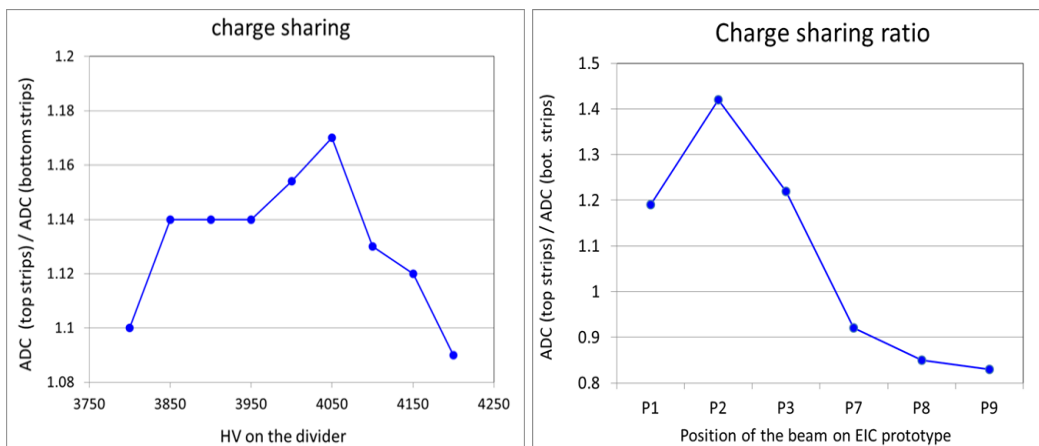
Figure 31 ADC charge ratio vs. HV applied on (left); Charge ratio vs. beam position on the prototype.

The plot on the right shows a strong non uniformity of the charge ratio at different locations in the chamber. This non uniformity can be explained by both the big variation of the signal to noise ratio at different location on the chamber because of the different strip length but also due to non-uniform electric field in the induction region caused imperfect stretching of the GEM foil or bending of the readout board due to the gas pressure. Ideas to improve the stretching is and induction gap uniformity are under investigation and will be implemented in the

Spatial resolution.

The spatial resolution was studied with 120 GeV proton beam data from the FTBF test beam. A detailed description of the FTBF Test Beam setup, beam condition as well as the analysis and results is going to be published soon in a forthcoming paper and only a short summary of the resolution calculation is given here. The setup at the FTBF test beam for the spatial resolution studies comprised three small (10×10 cm^2) standard triple GEM used as trackers. Two of the small GEM were located upstream the EIC-GEM prototype with respect to the beam and the third downstream. Simple least squared linear fit algorithm is used to fit the track. In order to measure the spatial resolution in x and y directions of the EIC-GEM prototype, we used the geometric mean method described in [4]. With this method, the resolution is the geometrical mean $\sigma = \sqrt{(\sigma_{incl} \times \sigma_{excl})}$ of respectively the width of inclusive residual and exclusive residual distributions of the measure cooordinated from the fitted track. For the inclusive residual, the data from both probed detector (the EIC-GEM prototype) and the tracking detectors (small GEM trackers) are used to get the fitted track whereas for the exclusive residual, only data from the tracking detectors are used for the fitted track.
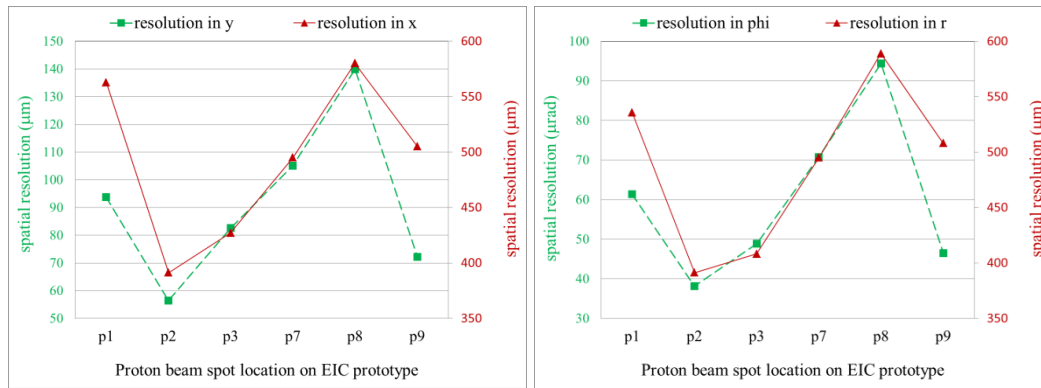
Figure 32 Position resolution at different location Cartesian (x,y) and polar coordinate (r,ϕ)

Figure 32 shows resolution for both cartesian coordinates x and y on the left plot and in polar coordinates r and φ on the right plot measured at different location in the chamber. In the Cartesian system, the resolution σ_y varies from 50 μm to 150 μm for y-coordinates from one position to another and is roughly 5 times higher for x-coordinates as expected because of the 12° angle between the top and bottom strips. σ_x varies between 350 μm to 550 μm. In the polar coordinates the variation shows similar pattern for both σ_φ and σ_r with a variation between 40 μrad to 100 μrad and 400 μm to 600 μm respectively. These are large variation in the position resolution from one point to the other that can be explained by the non-uniformity of the cluster size and charge ratio discussed in the previous sections. We believe that the non-uniform behavior could be corrected with some minor modification that we are planning to apply to the design of the second EIC prototype and its readout strip board.

Yale University group

3 Coordinate GEM

Further code development is in progress to refine the alignment procedures, the clustering algorithm and space-point calculation. In this regard we have benefitted greatly from the collaborative exchange of ideas and analysis techniques with the other groups in the collaboration who had GEM chambers under test in the test beam at Fermilab. We note that the very first pass analysis already has shown spatial resolution of ~100 μm which is quite good for 800 μm pitch. We expect to improve this number with the refinements indicated above.

Initial electrical tests on the 600 μm pitch boards indicate there may be a yield issue with the diagonal coordinate. This coordinate has many vias along each "strip." The failure of any single via will cause loss of signal from part of the strip. Indeed this is one of the features we planned to study with this research.

Hybrid Gain Structures for TPC Readout

Although funding just arrived we have none-the-less made some basic measurements for a 2GEM + MMG gain structure. We borrowed a MMG from RD51 and assembled a 10 cm x 10 cm 2 GEM + MMG chamber with pieces on hand. Figure 33 shows the setup we built to measure energy resolution and ion back flow (IBF). Initial tests have been done with this chamber. Two standard GEM foils are mounted above a MMG. The gas used (90%Ne, 10%CO_2), drift field, and overall gain (~2000) were chosen to be similar to the ALICE TPC. The radioactive source (^{55}Fe) intensity is adjusted to give an anode current of less than100 nA. The anode and cathode currents are both measured with the ratio giving the IBF. A small DAQ system with a calibrated pre-amp, shaper amp and DAC is used to measure the gain and resolution for the ^{55}Fe X-ray.
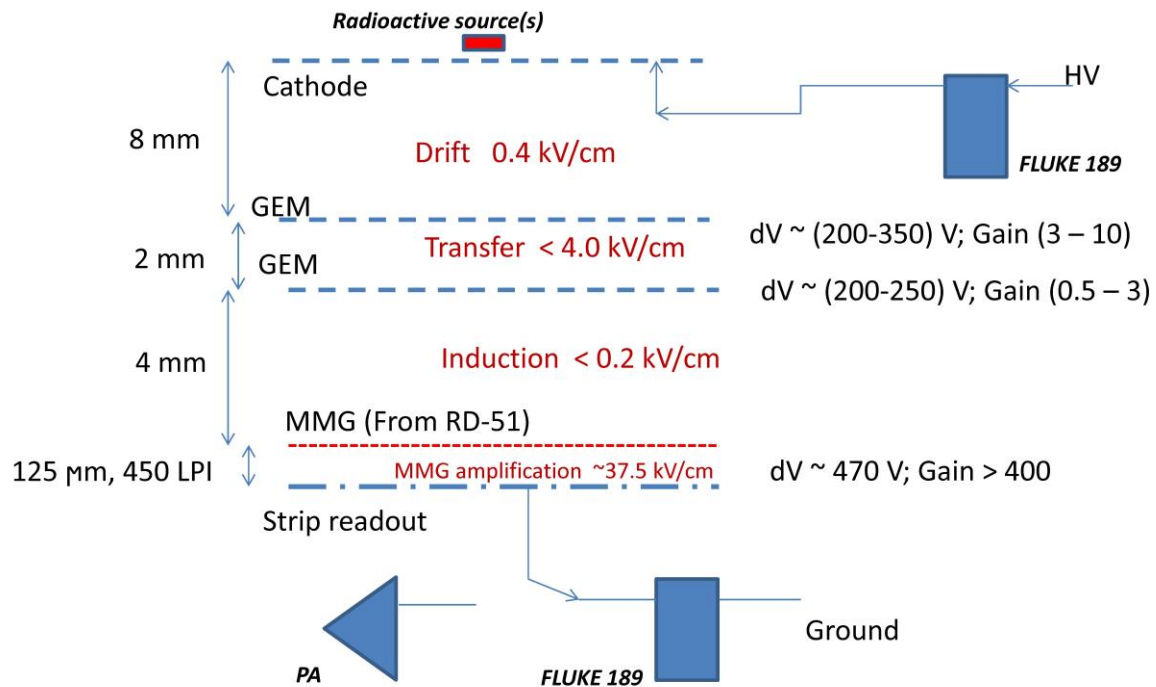
Figure 33 Chamber for measuring Ion Back Flow and energy resolution from a hybrid gain structure.

Table 1 shows the results of a voltage (gain) scan of the MMG, also varying the voltage (gain) of the top GEM to keep the total gain at ~2000. The fifth and seventh columns show the resolution (standard deviation for [55]Fe peak) and IBF (cathode current/anode current) for each setting. These results are very promising, indicating that an energy resolution better than 12% can be maintained while achieving IBF < 0.2%

WHAT WAS NOT ACHIEVED, WHY NOT, AND WHAT WILL BE DONE TO CORRECT?

Brookhaven National Lab group

The analysis of the Fermilab data taken with the Compass style readout board is essentially complete and we are now beginning to analyze the data with the chevron readout. This will be very valuable in understanding the response of the chevron pads that we plan to use in our TPC prototype detector. We expect that this analysis can be finished during the next several months, which will then complete the analysis of all of our current test beam data. We have submitted a contribution to the 2014 IEEE Nuclear Science Symposium which will take place in November of this year at which we plan to present all of our final results. We will then also submit a paper to the IEEE Transactions on Nuclear Science to publish these results.

We did not make as much progress on the design of the TPC prototype detector since most of our effort was focused on finishing our studies of the minidrift detector. However, now that that is nearly complete, we intend to turn our attention to be mainly on the TPC, and we expect that this will now progress at a much faster rate. We also have a new student that has joined our group (Michael Phipps) who worked with our collaborators at the Florida Institute of Technology and has excellent experience with GEM detectors, and also with TPC's from having worked on another TPC project. We expect that his involvement will greatly help to advance the project.

While the mechanical design and construction of the TPC prototype will include all provisions for installing the Cherenkov detector inside, the initial tests will be done with only the TPC portion. This is to make sure that this part works well first before dealing with the complication of adding the CsI GEM which requires special handling and will complicate the operation of the detector.

We have not yet identified a suitable set of readout electronics for the TPC, but we have several promising candidates. For our initial studies, we plan to use the CERN SRS system, which will allow us to study many of the properties of the TPC, but has limited capabilities in terms of measuring long drift times (< 1 μsec). However, we also have several Struck SIS 3300/3301 modules that can digitize up to 10 μsec, but we only have 24 channels of this readout. We have 128 channels of CAEN V1742 digitizers that utilize the DRS4 readout chip (providing sampling up to 5 Gsps), which will allow us to study such things as timing and pulse shape in great detail. We also expect to receive the first readout cards that use the new VMM2 chip designed by the BNL Instrumentation Division this summer, and we will certainly investigate that as a possible readout system as well. We are investigating the use of the GET TPC electronics, which has been widely used by other groups for small to modest sized TPCs, as a possible readout for our detector. Finally, we will be following the development of the SAMPA chip that is being developed to read out the ALICE TPC and is also being investigated for a TPC for EIC by our Livermore collaborators.

We did not upgrade the optics of our VUV spectrometer due to lack of funding. However, this will eventually be needed for developing the Cherenkov portion of our TPC prototype.

Florida Tech group

The tracking data taken at non-normal beam incidence angles with the 10cm × 10cm GEM detectors with radial zigzag readouts and the data taken with a 30cm × 30cm GEM detector with 30cm-long straight zigzag strips have not been analyzed, yet. The reason is that we have focused on analyzing the data taken with the large prototype first. The careful alignment of the tracker detectors and of the large prototype to the tracker proved to be a fairly complex and time-consuming task. The remaining analyses are next on our task list.

There was no magnet available at the FNAL test beam line, so we still lack a performance study of GEMs with zigzag readout in a magnetic field. Undergraduate students at Florida Tech have been refurbishing a 1T table-top magnet with 10cm diameter pole faces. We plan to measure at least basic parameters such as strip cluster sizes as a function of magnetic field by placing the small zigzag GEM detectors into this magnet and irradiating with radioactive sources.

Stony Brook University group

The charge division studies have been performed by an undergraduate student. The student identified the problem and implemented it into software code. The student has finished his studies after the spring semester ended at Stony Brook University and after writing his thesis the student left the group and the field. We are in the process of recruiting one or more students for the summer break who will be continuing the work on the studies. We are expecting that results will be obtained soon after and will design patterns of pads that will serve as a prototype and be tested with gas detectors and electronic readout systems.

University of Virginia group

We have focused our effort in the past months on the analysis of the data from test beam at Fermilab. The analysis required careful alignment of the EIC-GEM prototype with the GEM trackers to refine the residual distribution for resolution studies. We have also dedicated considerable effort to study the response function of strips readout and its impact on the resolution when using the center of gravity method used to calculate position coordinates from the cluster. This study is still ongoing and we are writing a paper on the final test beam results for publication in the NIM A peer-reviewed journal. Meanwhile we also have submitted an abstract to the 2014 IEEE Nuclear Science Symposium in November of this year to present the R&D for EIC forward tracking system and test beam results.

Though we have been exploring various ideas for the next EIC-GEM prototype design, we have not yet completed the design with all the improvements that we are planning to implement. With the analysis of the test beam data almost completed, we are going to focus our effort during the next 6 months into the design and construction of an EIC specific GEM prototype.

Yale University group

3 Coordinate GEM

Full electrical characterization of the 600 μm pitch boards remains to be done.

Progress Reports Future

WHAT IS PLANNED FOR THE NEXT FUNDING CYCLE AND BEYOND? HOW, IF AT ALL, IS THIS PLANNING DIFFERENT FROM THE ORIGINAL PLAN?

Brookhaven National Lab group

- Finish the analysis of the Fermilab test beam data and submit a paper on these results for publication.
- If funds are available, upgrade the beam optics of our VUV spectrometer in order to improve its sensitivity and resolution in the deep UV (below 140 nm).

Florida Tech group

Analysis: In addition to expanding the beam test data analysis to include other detectors, we want to attempt to refine the analysis for the large detector a bit further. Specifically, we plan to investigate if the strip response corrections can be fine-tuned some more to further improve the angular resolution of the large zigzag GEM.

We have started to prepare a publication containing the results presented here and in our previous report. The target journal is NIM A. We plan to send the paper out around October after the data analysis is completed.

Detector Design: As a new development that is somewhat different from the original plan and that is an outcome of discussions in the task force meetings mentioned above, Florida Tech and U. Virginia now plan to join forces with Bernd Surrow, et al., from the EIC RD2012-3 effort in designing and constructing the next detector prototype for the EIC forward tracker using entirely domestically sourced materials.

Currently, CERN is the only source in the world for large GEM foils. Our joint effort aims at making future production of an EIC forward tracker become independent of the schedule and capacity of the CERN workshop, which will have significant commitments to supply the upgrade projects of the LHC experiments (ALICE TPC, CMS forward muon, ATLAS muon upgrade) with large GEM foils and other MPGDs in the coming years. The key element for the success of such an effort will be to enable TechEtch to produce 1m-class GEM foils using the single-mask etching technique they have recently mastered.

Each of the three EIC groups brings complementary expertise to this joint forward tracker effort. Florida Tech has experience with constructing large GEMs without gluing and without spacers and with designing cost-effective readout boards; U. Virginia has experience with designing and constructing low-mass readout boards. Both groups are experienced in operating large chambers with the SRS readout. The Temple group has much experience with optical quality control of GEM foils. In addition, they are already designing a large GEM foil suitable for the actual radial range of $\sim 0.1m < r < \sim 1m$ of the EIC forward tracker.

The three groups agree that they will collaborate on the design work for the next EIC forward tracker prototype over the next 6-month R&D period. As a starting point for this joint effort, the groups will carefully review the specific requirements on the technical design of the forward tracker in light of recent simulation

results. Florida Tech plans to contribute by adapting the advanced design of the current prototype that enables detector construction without gluing and without spacers and that allows the detector to be reopened if needed. In addition, we will design an optimized zigzag-strip readout board for the new detector geometry and design. Aiwu Zhang will start working on these design tasks once he has completed the data analysis of the beam test data.

In the subsequent 6-month R&D period starting in spring 2015, the three groups plan to begin construction of the new prototypes. The key issue then will be to work with TechEtch on the production and testing of 1-m class GEM foils. At that point, we anticipate significant Non-Recurring Engineering (NRE) costs to be incurred because TechEtch will have to significantly upgrade their production facilities, e.g. larger etching tanks, to fulfil our orders for large GEM foils. We are currently working with TechEtch to get a precise cost estimate so that we can make an appropriate request for funding of this development effort at the January 2015 review meeting. We note that TechEtch has "unfortunately" (for us) expanded its workforce recently and does not qualify for SBIR funding anymore, so we would look to direct funding of this development from the EIC R&D effort. Clearly, having a domestic commercial source of large GEM foils available will have a positive impact on the broader U.S. experimental NP and HEP communities.

Hardware: Finally, we would also like to address a long-standing request from the reviewers regarding the long-term stability of large stretched GEM foils. Florida Tech undergraduates have recently built a 2m × 1.5m shielding box that allows the full-body irradiation of our trapezoidal GEM detector with an x-ray generator. Using that setup, we plan to measure the response of our 1m-long GEM detector at regular intervals, e.g. monthly, and over the long-term, i.e. at least for a year, to see if any response changes due to foil cracking or foil creeping are observed. This will require gain corrections for pressure and temperature variations, for which we request some small funds for T, P monitoring devices. In addition, we will be on the lookout for any increase in the sparking rate.

Stony Brook University group

We will continue working on the resistive charge division scheme and design appropriate test patterns of pads that will serve as prototypes for the readout with higher position resolution and at the same time reduced electronic channel count. The pattern will be ordered from and produced by an external provider. We will not be asking for funding within this round of proposals.

University of Virginia group

The largest GEM chamber for the EIC forward tracker would be 1.5 m long. A chamber of that dimension requires some fundamental R&D effort both in term of the GEM foil design and readout board approach. For the coming months, we have identified four important design ideas to drastically improve the construction as well as the performance of large size GEM detector for EIC forward tracker. We plan to build a new prototype to implement and study the ideas. We also formed a mini-collaboration with Florida Tech and Temple University dedicated on sharing ideas on the forward tracking GEM R&D for the EIC.

New ideas for design and assembly of an EIC-specific GEM prototype

We are investigating four ideas to improve the performances, facilitate the assembly procedure and provide more flexibility in term of replacing at later stage GEM foil if needed. The main improvements we are planning to implement are shown on Figure 34.
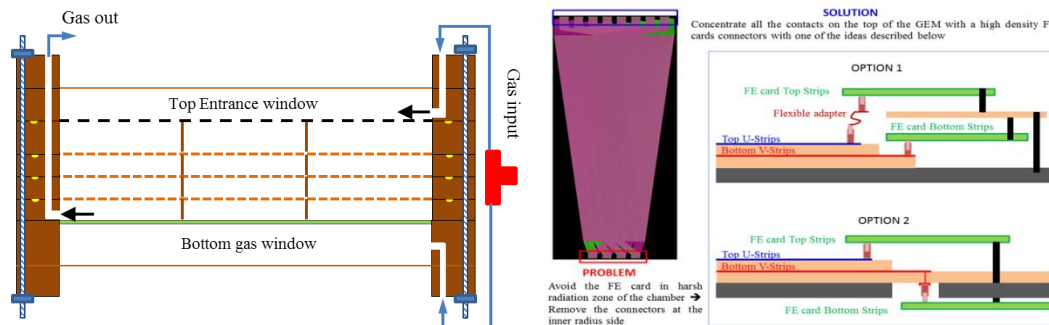

Figure 34 Design for a low-material re-"openable" GEM chamber (left) and new ideas for large 2D u-v strips readout board design for EIC GEM

The cartoon on the left shows a cross section of the new design for a light weight chamber where we replaced the honeycomb support used in the current prototype by a gas window closed by 25 μm thick Kapton foil. The gas flowing into this volume below the readout foil will counter-balance the pressure in the other part of the chamber to allow a uniform gap in the induction region.

Another major modification is that we no longer plan to glue the framed GEM foil together. Though the GEM foils are still going to be mechanically stretched and glued to the support frame with spacer, the framed GEMs and drift cathode will be stacked and screwed to on the readout board and the gas tightness will be provided by O-ring structure on each frame. In the current design where all the frames are glued together, it is impossible to replace a faulty GEM or readout board after the final assembly. This new assembly scheme that we proposed is an excellent compromised solution between our current technique with narrow support frames therefore minimized dead area and the technique used at Florida Tech with no inner spacer in the chamber and re-"openability".

The third modification we want to study is summarized in the cartoon on the right of Figure 9. On the current EIC GEM prototype, the Front-End (FE) readout electronics are connected the 2D readout board of the chamber at both the inner radius and the outer radius sides of the chamber. This option was chosen to avoid having to connect FE cards on the sides of the chamber in order to minimize the dead area when the GEM modules are arranged together into a disk layer of the forward tracking detector. But FE cards at the inner radius of the chamber will be exposed to a very high radiation dose because of the proximity to the beam line. We propose to explore a new idea to enable all strips of both u and v strip layers to be read-out from the outer radius side of the chamber. The proposed concept illustrated in, calls for two layers of FE cards at the outer radius side of the chamber and allows to further reduce the pitch and the width of the readout strips and therefore improved the position resolution by reducing the signal to noise ratio.

We are also planning interested in implementing the excellent study by Craig Woody s group at BNL exploiting the mini-drift capability of the GEM detector signal as way to maintain an excellent resolution at large incoming particle angle. Bob Azmoun from this group has demonstrated on a small 10×10 cm² GEM chamber with Cartesian strips readout, that one can obtain a very good an uniform spatial resolution over a wide range of incoming particle angle by combining both the center of gravity method to get the cluster position at lower angle and a mini TPC-like track reconstruction at large angle. We plan to learn from Craig's group and expand their study to large size 2D u/v strip readout and implement the reconstruction algorithm developed by the group.

Collaboration with Florida Tech and Temple University for EIC Forward Tracker R&D.

As stated by Marcus Hohlmann in the Florida Tech section, Univ. of Virginia, Florida Tech are joining forces with Bernd Surrow in to share their respective expertise in the design and construction of next EIC-GEM prototype. The goal is to work on a common design or at least a design that share some common features between the three groups with each group focusing on a specific R&D aspect that it wants to develop. So as an illustration, we at UVa are more interested in developing a light-weight, re-"openable" GEM with improved 2D u/v readout strips design as described above.

One critical aspect of this collaboration is the interest and focus of the three groups in promoting and supporting domestic production of large size GEMs foil and 2D readout board through close collaboration with TechEtch. A first step will be for the three groups to work with TechEtch on the production and testing of 1-m class GEM foils that might be used to assemble the next EIC-GEM prototype. Having a chamber that could be re-opened would then provide a way for direct comparison between GEM chamber built using CERN foils and TechEtch foils in addition to the optical test of single GEM foil capability already available at Temple University.

Yale University group
3 Coordinate GEM

The major activity for the next period will be continuing analysis of the data collected in the test beam run at Fermilab. Analysis activities going forward we will include finalizing chamber alignment procedure, optimizing the clustering algorithm, optimizing the space-point calculation and writing a paper on the results.

The coordinate measuring machine purchased by the Yale ATLAS group has just been upgraded to include a touch probe. We expect to use this during the next period to automate or semi-automate full electrical characterization of the 600 μm pitch boards. This should give us the data needed to know if 600 μm pitch is viable with present technology for the 3-coordinate scheme.

CENTRAL TPC R&D

We continue our R&D on TPC designs as the optimal low-mass detector to provide excellent tracking at mid-rapidity, -1<y<1, and limited particle identification of hadrons with full azimuthal coverage.   Although TPCs have been in use in high energy and nuclear physics experiments for more than 25 years, their use in high rate environments is new, and a focused R&D effort is needed to insure that an EIC TPC can meet the current expected luminosity for the EIC is 1033cm-1s-1, corresponding to a collision rate of 30–60 kHz, depending on the collision energy. The primary challenge in a high rate environment is to achieve adequate gas gain while limited the ion back flow to levels that do not hamper the momentum resolution through large electric field distortions. The Yale group will continue R&D on hybrid gain readouds (GEM and MicroMegas). In addition, we plan to investigate a new gating grid design proposed by Howard Wieman. We will also explore options for electronics readout, a dominant cost driver for most TPCs. This will involve performing small-scale tests with the SAMPA ASIC, currently under development for the ALICE TPC upgrade.   R&D on the gating grid and electronics will be led by the LLNL and WIS groups, who have recently joined this consortium. The BNL group will continue R&D on a hybrid TPC/Cerenkov detector.

We propose to begin research and development on the critical path items of a Time Projection Chamber (TPC) for the Electron Ion Collider (EIC). We will explore an innovative gating grid design to reduce ion backflow and to make quantitative comparisons among different gas multiplication methods. We will also begin small scale tests to evaluate the SAMPA ASIC being developed for ALICE to determine if this design will meet the requirements for the EIC, thereby reducing or eliminating the cost of a separate electronics design phase in the future.

TPC/Cerenkov Hybrid (BNL)

- Finalize the design of the TPC/Cherenkov prototype detector and begin construction. Construction could be completed during the second half of this year.
- Study various readout electronics for the TPC. Identify which system would be best for the full readout of the TPC section of the detector.
- Continue studies of various gas mixtures for the TPC to determine which is best in terms of speed, diffusion, and charge collection efficiency.
- Continue studies of ion back flow to reduce space charge effects

Hybrid Gain Structures for TPC Readout (Yale)

The results shown above are very promising. We plan to make similar measurements varying all voltages and fields, measurements with different gas mixes, and possibly varying gap distances.   Further measurements will be made with a heavily ionizing source to characterize the stability of the gain structure against sparking.

As proposed, we will also order several small MMG chambers to investigate different fabrication techniques. In particular, it should be possible to provide support for the MMG mesh using ridges running in the space between pad rows on the readout plane. This should minimize loss of signal near the support structure. We

also will investigate segmenting the MMG mesh to minimize the energy in a discharge and study spark protections schemes to minimize possible damage to electronics and dead time from discharges.

MMG, V	<GA>, MMG	dV, GEM 2, V	<GA> (x e3)	Sigma /Mean, %	Anode current, nA	IBF, %
435	265	260	1.85	10.2	14.0	0.28
445	339	250	1.90	10.6	14.5	0.25
455	411	240	1.95	11.1	15.2	0.21
465	519	230	1.99	11.8	15.9	0.18
475	656	225	2.05	12.1	18.3	0.16
485	838	220	2.15	11.9	19.4	0.14

Drift – 0.4 kV/cm;   dV GEM 1 – 210 V;   Transfer – 3.0 kV/cm; Induction – 0.08 kV/cm

Table 1 IBF and energy resolution of various MMG gains. The top GEM (GEM 2) gain is also varied to keep the total chamber gain ~2000. Parameters kept constant are listed below the table. The working gas for this scan is 90% Ne, 10% CO_2.

Layered Gating Grid

The traditional method for reducing ion backflow in a TPC is to use a gating grid which when closed terminates the electric field lines above the readout plane, thereby inhibiting gas multiplication and limiting the buildup of positive ion space charge in the TPC. The gating grid limits the readout rate to the inverse of the sum of the electron drift time of the vessel and the ion drift time in the gating grid region. For a 2-meter chamber, electron drift times alone are in the range of 10–40 µs, depending on the choice of drift gas, and the TPC has one or two drift regions. This is on the edge of the anticipated average collision rate, but the addition of the ion drift time in the range of ~100 µs pushes the readout rate beyond this range.   For the the ALICE TPC upgrade [6], which is striving for a similar collision rate of 50 kHz but much higher track densities, the standard gating grid is not an option, and multi-layered Gas Electron Multipliers (GEMs) are being developed to limit the ion backflow. For the lower track densities of the EIC, the situation is more nuanced, and a significant improvement to gating grid concept could make this option viable. An innovative gating grid design was recently proposed by Howard Wieman during a review of the ALICE TPC upgrade. We propose to work with Howard Wieman on simulations and small-scale bench tests to test this idea in the context of an EIC TPC as the first component of our R&D effort in 2015.

This new gating grid idea is shown in Figure 35. In this configuration, the conventional single layer gating grid is stacked four layers deep, enabling a larger fraction of the ions to be cleared in each cycle. This idea was proposed to supplement the multi-layer GEM readout in the ALICE TPC, but for the EIC one could consider reducing the number of GEM layers, using a single layer Micro-Mesh Gas Amplifiers (MicroMegas), or potentially using a conventional pad readout, depending on the efficacy of the new design. We propose to test this gating grid concept through simulations and small-scale tests in the laboratory.
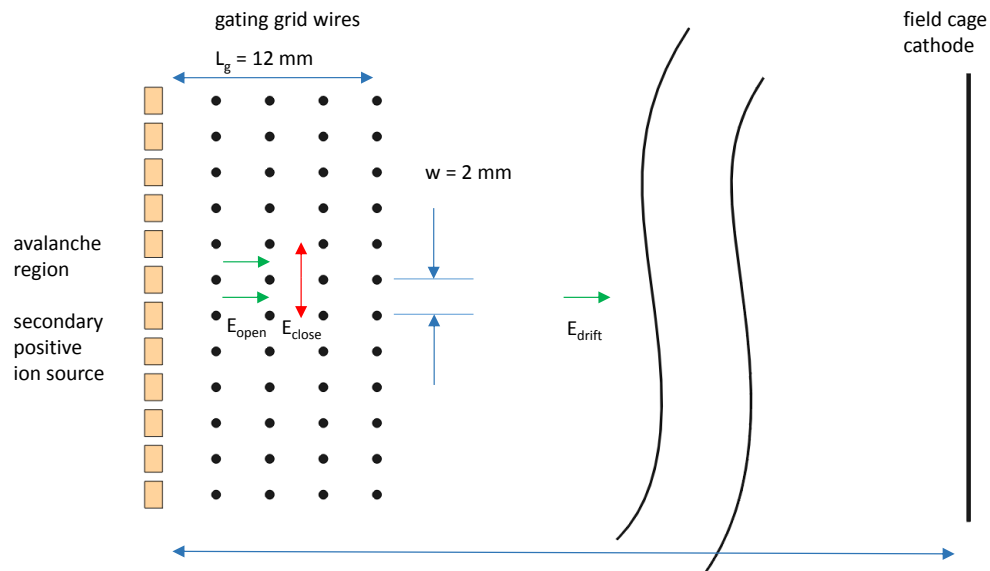
Figure 35 Schematic of layered gating grid design to reduce ion backflow in EIC TPC.

Simulations (LLNL)

To begin testing this gating grid concept, we will simulate the full electric field and layered gating grid performance using Garfield combined with Elmer or Magboltz. The simulations will be used to estimate field transparency, clearing time, ion leakage, and other operational parameters. This work will be performed by a postdoc at LLNL working 25% time under the guidance of Howard Wieman at LBNL. Results of the simulations will be used to guide experimental tests to be performed at the Weizmann Institute of Science.

Laboratory Tests (WIS)

A small test chamber will be used to field test the layered gating grid design. These results will serve the benchmark the simulations, and will be used to estimate the impact of field distortions on the momentum resolution of the TPC. These measurements will also be compared to measurements for GEM and MicroMegas readouts. In general, the ion backflow might be governed by several parameters, namely: gas mixture, pressure, detector gain, hole diameter in case of GEM or lines per inch in case of MicroMegas, the

combination of the drift, transfer and induction fields, number of GEMs used for the amplification element and asymmetry in the voltages applied across each GEM. The Heavy Ion Group at the Weizmann Institute of Science will perform the ion backflow measurements as a function of the parameters mentioned above.

TPC Electronics Readout (LLNL)

Historically, the cost of electronics procurements comprise between one third and one half the total cost of a TPC [7, 8]. The chip design process will drive these costs significantly higher, but these additional costs can be reduced or even eliminated by working with an existing chip design. The SAMPA chip, currently being developed for the ALICE TPC upgrade, is a third generation design that builds upon the PASA/ALTRO and S-ALTRO ASICs used by the STAR and ALICE TPCs. The SAMPA ASIC, which provides increased bandwidth and integration with reduced power, appears to be an optimal choice for an EIC TPC, but it is essential that we perform our own tests. By performing early tests and making contact with the SAMPA design team in Sao Paulo we will be able to influence the design in the event that changes are required. This group is about to begin its first component run in the fall of 2014. We propose to participate in the second phase ASIC run in order to procure a small sample of integrated ASICs for testing by the TPC Tracking Consortium.

The SAMPA ASIC design is led by the Sao Paulo group, which worked previously on the 16-channel PASA/ALTRO and S-ALTRO chips. SAMPA will integrate 32 channels of readout, beginning with positive/negative polarity Charge Sensitive Amplifiers that output semi-Gaussian voltage signals that are digitized by 10-bit 10 Msample/s ADCs. Signals are then processed digitally to remove distortions and transmitted over four 320 Mb/s e-links for a maximum rate of 1.28 Gbs.

The first run will deliver block components for the preamp, shaper, ADC, and DSP for testing by the Sao Paulo group. We propose to participate in the second run, procuring a small sample of integrated ASICs for use by the EIC TPC group. This run is expected to take place early in 2015. Testing will be overseen by a postdoc at LLNL who will supervise the graduate students at UC Davis who will perform actual testing. The full set of tasks for testing electronics is:

1. Work with electronics group to get packaged chips, board design, and associated documentation.
2. Build test boards and assemble with test chips.
3. Write software to interface with the chip.
4. Test the interface to the chip and exercise the functions.
5. Measure chip performance, power, noise, cross talk, etc...
6. Report back to the electronics group and the EIC on the readiness of chip design.

The budget request is limited to the cost of the parts and board assembly. Effort for the LLNL postdoc (25%) and UC Davis graduate student (50%) will be covered by existing base funding at their respective host institutions.

WHAT ARE CRITICAL ISSUES?

Brookhaven National Lab group

Finish the analysis of the test beam data for the minidrift detector and publish a paper on the results.

Finish the design and complete the construction of the TPC/Cherenkov prototype detector.

Identifying suitable readout electronics for testing the prototype.

Florida Tech group

Much of the previous work presented above and of the work planned relies heavily on our EIC hardware post-doc Aiwu Zhang, who has been doing a fantastic job in his first year on the project. He is currently funded by this effort until Sep 30, 2014. Continued funding for his salary and the timely arrival of the funds at the institution are absolutely critical to the proposed work.

Enabling TechEtch to produce 1m-class GEM foils is critical for developing an EIC forward tracker.

Stony Brook University group

Finalizing the studies for a charge division scheme.

University of Virginia group

Need to perform critical R&D and design studies to improved performances, construction, handling of EIC requirement specific large size GEM prototype.

Collaboration effort from UVa, Florida Tech, and Temple U for the support, characterization and validation of domestic production of large area GEM foils by TechEtch.

Yale University group

3 Coordinate GEM

As discussed above a critical issue is the reliability of fabrication of the finer pitch boards and whether it is possible to scale this technique to larger readout boards.

Hybrid Gain Structures for TPC Readout

The goal of this research is to produce a gain structure for TPC's that maintains good energy resolution and reduces ion backflow to a level that allows continuous sensitivity of the TPC. Producing a gain structure optimized for energy resolution, minimum ion backflow with good stability is the critical issue.

Additional information

LLNL and WIS

Personnel and Facilities

TPC Group at Weizman Institute of Science

The Heavy Ion Group at the Weizmann Institute of Science (WIS) has a long history and experience in designing and building the various gaseous detectors for CERN and RHIC heavy ion experiments. In particular this experience includes the TPC read-out chambers construction for the CERES/NA45 experiment at CERN SPS, Pad Chambers, and GEM based Hadron Blind Detector for the PHENIX experiment at RHIC. In addition to the experience, the WIS group has a fully equipped lab, including the following items:

1. Laminar flow table inside clean room   and gas mixture system

2. Scalable Readout System (SRS) purchased at CERN

3. RCDAQ Linux based software for SRS developed at BNL

4. CAEN High Voltage Main Frame and a number of power supplies

5. 40 kV power supply for the TPC test cell

6. NIM modules for a fast electronics

7. Vacuum equipment including turbo pump

The people from the Heavy Ion Group of the Weizmann Institute of Science who will work on this TPC R&D are Sasha Milov (Faculty), Ilia Ravinovich (Faculty), Sourav Tarafdar (PostDoc) and a number of students. Graduate students will also join this effort as it moves towards the design and construction of a prototype TPC for the EIC.

TPC Group at LLNL

The LLNL heavy ion group has significant experience in the design, construction, and operation of TPC detectors. The TPC lab at LLNL is fully equipped with a gas system, test vessel, and readout system. The group has experience in building MicroMegas and LEM gas gain systems, as well as the custom design of readout electronics [6]. The group has also developed software tools needed for calibration, tracking, and physics analysis. Past projects include a Hydrogen TPC for directional neutron detection [10] and a negative ion TPC with oxygen carrier that achieved single electron counting [11].

The LLNL TPC group is currently operating and analyzing data from a TPC in the Neutron Induced Fission Fragment Tracking Experiment (NIFFTE) [12]. The NIFFTE TPC is a two chamber MicroMegas TPC designed to make precision cross-section measurements at LANSCE. A cut-away of the TPC is shown in .
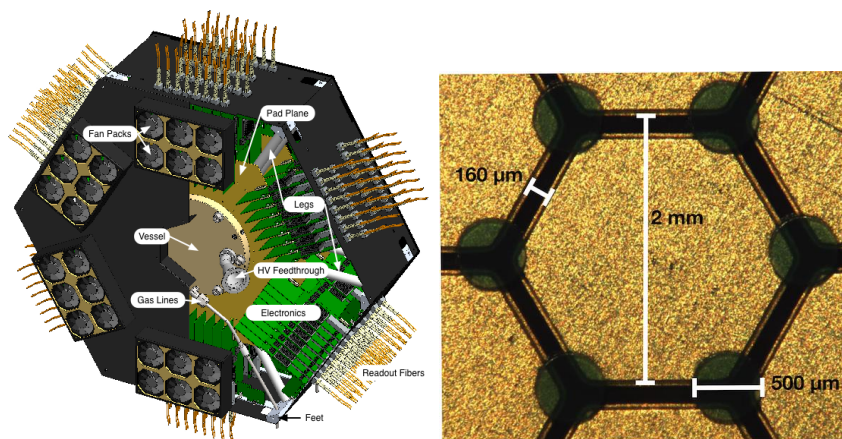
Figure 36 : (Left) The NIFFTE fissionTPC with part of the cover removed. (Right) Micrograph of MicroMegas pad and pillar. The gold colored hexagon at the center is one pad and the close pack tessellation of the neighbor pads with 160 μm gaps between pads is also visible. The green circle at each hexagon point is a 75 μm tall insulating pillar to support the mesh.

TPC Collaborators

Howard Wieman, LBNL designed the STAR TPC [7], and has been an innovator in TPC design for many years. Howard will serve as a consultant on the simulations and bench tests of his layered gating grid design.

The UC Davis heavy ion group, led by Dan Cebra, has significant experience in all phases of TPC design, construction, calibration, and data analysis. The UC Davis group will contribute lab space and graduate student effort as needed to test and document the SAMPA ASICs.

Budget Justification

The WIS TPC group requires funding support for the mechanical design and technical support and in order to purchase the amplification detector elements for testing the layered gating grid, and measuring ion backflow compared to GEM and MicroMegas. Funding for the LLNL group will cover 25% postdoc effort for simulations of the layered gating grid. The remaining funding will be used to procure a small number of SAMPA ASICs, and to purchase and populate boards for testing. The full request and breakdown is listed in Table 2.

Funding Requests

Brookhaven National Lab group

We are not requesting any additional funds for the second half of FY 2014. However, if funds are available, we would request $15k to upgrade the optics of our VUV spectrometer.

Florida Tech group

The budget requested by Florida Tech for FY15 is listed in the following table (all items in k$).

Florida Tech FY 15 Budget Request				
	Jun-14	Jan-15	**Total**	**Comments**
Forward tracking: Large-area GEM detectors				
Fully loaded personnel (Post-doc Aiwu Zhang)	90	0	90	12 months support
Undergraduate summer support	0	4	4	
GEM chamber parts and readout boards	0	30	30	
Travel	3	3	6	EIC inst.; conf.
Supplies & Materials	3	5	8	T,P monitor; gas
Overhead not included in post-doc salary	3	4	7	
Total	**99**	**46**	**145**	

The salary request for post-doc Aiwu Zhang covers the 12-months FY15 period from Oct 1, 2014 to Sep 30, 2015. Given the typical delay of a few months until funds arrive at the institution after budget approval, it is critical that these salary funds be allocated in July 2014 so that they arrive in time for renewal of Aiwu's contract before Oct 1, 2014.

LLNL and WIS groups

Table 2 Cost breakdown for FY15 TPC R&D

Task	Cost
Layered Gating Grid	**$75k**
Simulation	$35k
Mechanical design	$15k
Components	$10k
Technical Support	$15k
SAMPA Testing	**$43k**
ASIC run	$35k
Boards	$3k
Assmbly	$5k
Total	**$118k**

Stony Brook University group

We are not requesting any additional funds for the second part of FY2014.

University of Virginia group

Requested budget by UVa for FY2014:

Item	Item cost ($)	Quantity	Total ($)
GEM foils	2000	4	8000
Readout board	3000	1	3000
Spacer frames	3000	1 set	3000
Material and supplies (Gas, cables, mounts, shipping goods …)	3000	1 set	3000
Mechanical Stretcher	5500	1	5500
Engineering & Technical support	7500		7500
Travel to CERN	5000		5000
Overhead	7250		7250
Fringes	2500		2500
Total			**45000**

Yale University group

We are not requesting any additional funds for the second part of FY2014.

8.

9.

10.

11.

12.

13.

14.

References

[1] M. Villa, Developing and evaluating new micropattern gas detectors, Dissertation, U. Bonn, CERN-THESIS-2013-284 (2014).

[2] S. Martoiu et al., "Front End Electronics for the Scalable Readout System of RD51", in 2011 Proc. IEEE Nucl. Sci. Symp., pp 2036-2038

[3] RD51 Collaboration, http://rd51-public.web.cern.ch/rd51-public/

[4] DATE & AMORE: LHC ALICE Experiment DAQ & Monitoring Software,

https://ph-dep-aid.web.cern.ch/ph-dep-aid/

[5] T. Alexopoulos et *al.*, "*Examining the Geometric Mean Method for the Extraction of Spatial Resolution*", JINST 9 P01003 (2014)

[6] ALICE Collaboration, Technical Design Report for the Upgrade of the ALICE Readout and Trigger System, ALICE-TDR-015 November 4, 2013.

[7] STAR Collaboration, The STAR Conceptual Design Report, https://drupal.star.bnl.gov/STAR/starnotes/public/sn0499 , June 1, 1992.

[8] ALICE Collaboration, ALICE Technical Design Report of the Time Projection Chamber, CERN / LHCC 2000001, December, 1999.

 [9] Heffner, M., et al., IEEE Trans. Nucl. Sci. 60, 2196 (2013).

[10 Bowden, N.S., et al., Nucl. Instr. Meth. in Phys. Res. A 642, 153 (2010).

[11] Sorensen, P., et al., Nucl. Instr. Meth. in Phys. Res. A 686, 106 (2012).

[12] Heffner, M. et al. [NIFFTE], arxiv.org:1403.6771